Hindawi Publishing Corporation
Journal of Diabetes Research
Volume 2013, Article ID 143515, 5 pages
http://dx.doi.org/10.1155/2013/143515

Clinical Study

Impact of Serum Retinol-Binding Protein 4 Levels on Regulation of Remnant-Like Particles Triglyceride in Type 2 Diabetes Mellitus

Naoto Yamaaki,[1] Kunimasa Yagi,[1] Junji Kobayashi,[2] Atsushi Nohara,[1] Naoko Ito,[1] Akimichi Asano,[1] Kaoru Nakano,[1] Jianhui Liu,[1] Takuya Okamoto,[1] Yukiko Mori,[1] Azusa Ohbatake,[1] Satoko Okazaki,[1] Yoshiyu Takeda,[1] and Masakazu Yamagishi[1]

[1] *Department of Internal Medicine, Graduate School of Medical Science, Kanazawa University, 13-1 Takaramachi, Kanazawa 920-8640, Japan*
[2] *Department of General Medicine, Kanazawa Medical University, 1-1 Daigaku, Uchinada, Kahoku 920-0293, Japan*

Correspondence should be addressed to Kunimasa Yagi; diabe@med.kanazawa-u.ac.jp

Received 25 December 2012; Accepted 12 February 2013

Academic Editor: Aristidis Veves

Background. Although retinol-binding protein 4 (RBP4) associates with insulin resistance and remnant-like particles triglyceride (RLP-TG) elevated in the insulin resistant state, few data exist regarding the relationship between RBP4 and RLP-TG. *Subjects and Methods.* The study included 92 Japanese type 2 diabetic mellitus (T2DM) male patients (age 60.5 ± 13.6 years, body mass index (BMI) 24.7±4.1 kg/m^2, waist circumference (WC) 88.4±10.7 cm, and HbA1c (NGSP) 7.2±1.9%). Patients on medications affecting insulin sensitivity, including fibrates, biguanides, and thiazolidinedione, were excluded. Visceral fat area (VFA) and subcutaneous fat area (SFA) were measured by computed tomography. *Results.* RBP4 levels showed a significant positive correlation with RLP-TG (r = 0.2544 and P = 0.0056), TG (r = 0.1852 and P = 0.041), RLP-TG/TG (r = 0.23765 and P = 0.0241), and age (r = −0.2082 and P = 0.0219), although there was no significant correlation with VFA, SFA, adiponectin levels, or homeostasis model of assessment insulin resistance (HOMA-R). Multiple regression analysis revealed that RBP4 was an independent determinant of RLP-TG (P = 0.0193) but was not a determinant of TG. *Conclusions.* RBP4 correlates positively with serum RLP-TG independent of fat accumulation in T2DM. RBP4 may regulate remnant metabolism independent of glycemic control in T2DM.

1. Introduction

Retinol-binding protein 4 (RBP4) was originally identified as a signal molecule, which transfers the intercellular signals for insulin resistance [1]. Previous clinical studies have reported that RBP4 is associated with the extent of systemic insulin resistance and obesity [2, 3]. RBP4 has been shown to significantly correlate with clinical features relating to insulin resistance and metabolic syndrome, including hyperlipidemia and hypertriglyceridemia [4]. Furthermore, recent studies have shown that RBP4 mainly correlates with dyslipidemic profiles in type 2 diabetes, especially in terms of hypertriglyceridemia.

The retention of remnant lipoproteins is known to frequently occur in the insulin resistant state and in metabolic syndrome. Impaired remnant metabolism is one of the "residual cardiovascular risk factor" for atherosclerosis [5]. Remnant clearance is retarded in insulin resistant type 2 diabetics resulting in cardiovascular damage [6]. Even though the cardiovascular risk associated with metabolic syndrome has been well established, few data exist concerning the relationship between RBP4 and lipoprotein remnants such as remnant-like particles triglyceride (RLP-TG). Therefore, we are investigating the relationship between RBP4 and serum lipoprotein levels, including RLP-TG, in Japanese diabetic patients.

2. Patients and Methods

2.1. Patients. This study was approved by the ethical committee of Kanazawa University. Informed consents were

obtained from all subjects. All patients were recruited from Kanazawa University Hospital and its satellite hospital. Of 860 outpatients with type 2 diabetes mellitus, a total of 92 Japanese diabetic men (age 60.5 ± 13.6 years) with their agreement of the computed tomography were included in this study.

Patients on medications affecting the individual insulin sensitivity, including fibrates, biguanides, and thiazolidinedione, were excluded from this study [7, 8]. Patients with other endocrine diseases or significant renal or hepatic disease were also excluded. Obesity was defined as body mass index (BMI) $\geq 25\,kg/m^2$, based on the criteria of the Japan Society for the Study of Obesity [9]. Diabetes mellitus was diagnosed according to World Health Organization criteria [10] and/or receiving medications for diabetes mellitus.

2.2. Laboratory Measurements. BMI was calculated as weight (kg) divided by height (m) squared. Waist circumference (WC) at the umbilical level was measured in the exhalation phase of respiration while standing.

Venous blood samples were performed after a 12-hour overnight fast. Total cholesterol (TC) and triglyceride (TG) were determined by enzymatic methods, and high-density lipoprotein cholesterol (HDL-C) levels were measured by a polyanion-polymer/detergent method. RLP isolation was based on the removal of apo A-I-containing particles and most apo B-containing particles, using an immunoseparation technique, which has been shown to leave remnants of both intestinal and hepatic origin in the unbound fraction. Briefly, monoclonal antibodies to apo A-I and specific monoclonal antibodies to apo B, which do not recognize partially hydrolyzed, apo E-enriched lipoprotein remnants, were immobilized on agarose gel. RLP-TG concentrations were measured in the FHS plasma aliquots that had been frozen at −80°C until the time of analysis. Plasma was incubated with the gel for 2 hours, after which the gel, containing the bound (non-RLP) lipoproteins, was precipitated by low-speed centrifugation. Triglyceride concentrations were then measured in the unbound supinates. Blood glucose was measured with the glucose oxidase method and HbA1c by high-pressure liquid chromatography. Plasma adiponectin levels were measured with an enzyme-linked immunosorbent assay kit (Otsuka Pharmaceutical Co., Tokushima, Japan), and serum RBP4 was measured with Human RBP4 Competitive ELISA kit (Adipogen, Seoul, Republic of Korea).

It is well known that RLP-TG has strongly correlated with TG, which represents both overproduction and catabolism of VLDL. This suggests that RLP-TG levels can reflect VLDL overproduction. Therefore, we examined RLP-TG/TG ratio as the focused index for remnant catabolism. Homeostasis model of assessment insulin resistance (HOMA-R) is calculated using the following formula: fasting glucose (mg/dl) × fasting insulin (μU/mL)/405.

2.3. Body Fat Distribution. All subjects underwent computed tomography (CT) at the umbilical level to measure cross-sectional visceral fat area (VFA) and abdominal subcutaneous fat area (SFA) using Fat Scan (N2 System Corp, Osaka, Japan) [11]. VFA/SFA ratio was calculated as VFA divided by SFA.

Table 1: Clinical characteristics of the study subjects.

Age (years old)	60.5 ± 13.6
Body mass index (kg/m^2)	24.7 ± 4.1
Fasting blood glucose	130.5 ± 33.5
HbA1c (NGSP) (%)	7.2 ± 1.9
Total cholesterol (mg/dL)	203 ± 43
Triglyceride (mg/dL)	165 ± 155
RLP-triglyceride (mg/dL)	34.4 ± 45.4
HDL-cholesterol (mg/dL)	51 ± 16
LDL-cholesterol (mg/dL)	118 ± 30
RBP4 (μg/mL)	60.4 ± 35.0
Adiponectin (ng/mL)	6.84 ± 7.09
HOMA-R	2.88 ± 2.92
Waist circumference (cm)	88.4 ± 10.7
Visceral fat area (cm^2)	110.6 ± 53.5
Subcutaneous fat area (cm^2)	138.4 ± 75.2
Treatments for diabetic subjects	
Sulphonylureas	16
Glinides	12
Alpha glucosidase inhibitors	17
Insulin injection	10

All data were indicated as mean ± SD.

2.4. Statistical Analysis. All data are shown as mean ± SD. Continuous variables were compared by ANOVA after being adjusted for age, BMI, and sex. All statistical analyses were conducted with JMP ver. 10.0.2 for Macintosh OSX (SAS institute, NC, USA). A P value of less than 0.05 was considered statistically significant.

3. Results

Baseline clinical characteristics of the patients are shown in Table 1. Our previous report showed that poorly controlled type 2 diabetic men had more unfavorable lipid profiles than women, thus resulting in decreased lipolysis of plasma TG-rich lipoproteins [12]. Therefore, only type 2 diabetic men were enrolled in this study.

Relationships between RBP4 and other clinical parameters were shown in Table 2. RBP4 showed significant positive correlation with TG ($r = 0.1852$ and $P = 0.041$) (Figure 1(a)), RLP-TG ($r = 0.2544$ and $P = 0.0056$) (Figure 1(b)), WC ($r = 0.1919$ and $P = 0.0336$), and negatively correlated with age ($r = -0.2082$ and $P = 0.0219$). RBP4 also showed good correlation with RLP-TG/TG ($r = 0.2376$ and $P = 0.0241$) (Figure 1(c)). Importantly, there was no significant correlation between RBP4 and HOMA-R.

RLP-TG showed positive correlation with TC ($r = 0.2894$ and $P = 0.0017$), TG ($r = 0.6732$ and $P < 0.0001$), HbA1c ($r = 0.3506$ and $P = 0.0011$), HOMA-R ($r = 0.3527$ and $P = 0.0054$), RBP4 and negative correlation with age ($r = -0.3377$ and $P = 0.0003$), and HDL-C ($r = 0.3682$ and $P < 0.0001$).

Table 2: Pearson correlation coefficients in the 92 patients with type 2 diabetes mellitus.

	RBP4	TG	RLP-TG
RBP4	—	0.1852*	0.2544#
Triglyceride (TG)	0.1852*	—	0.6732$
Remnant-like particle TG (RLP-TG)	0.2544#	0.6732$	—
Age	−0.2082*	−0.2810#	−0.3337†
BMI	0.1433	0.0290	0.0824
Total cholesterol (TC)	0.1729	0.4297$	0.2894#
HDL-C	0.0179	−0.3663$	−0.3682$
LDL-C	0.1047	0.1531	0.0292
Fasting plasma glucose	0.1214	0.1468	0.1794
HbA1c	0.1268	0.3054#	0.3506#
Visceral fat area (VFA)	0.1386	0.1295	0.1537
Subcutaneous fat area (SFA)	0.1559	0.0225	0.0460
Waist circumference (WC)	0.1919*	0.0427	0.0976
Adiponectin	0.0842	0.0857	0.1114
HOMA-R	0.0923	0.1670	0.3527#

TG and RLP-TG were logarithm transformed. *$P < 0.05$; #$P \leq 0.01$; †$P \leq 0.001$; $$P \leq 0.0001$.

Table 3: (a) Multiple regression analysis with RLP-TG as a dependent variable and (b) Multiple regression analysis with TG as a dependent variable.

(a)

Factors	Standard error	t	p (prob > t)
Age	0.005372	−3.47	0.0008*
RBP4	0.001999	2.39	0.0193*
VFA	0.001597	1.87	0.0649
Adiponectin	0.010075	−1.59	0.1154
BMI	0.034605	−0.36	0.7208
SFA	0.001799	−0.23	0.8218

(b)

Factors	Standard error	t	p (prob > t)
Age	0.004836	−3.59	0.0006*
VFA	0.001434	2.40	0.0189*
BMI	0.031260	−1.64	0.1044
RBP4	0.001792	1.46	0.1485
Adiponectin	0.009033	−1.39	0.1687
SFA	0.001654	−0.19	0.8494

TG showed positive correlation with TC ($r = 0.4297$ and $P < 0.0001$), RLP-TG, HbA1c ($r = 0.3054$ and $P = 0.0042$), negative relationships with age ($r = -0.2810$ and $P = 0.0023$), and HDL-C ($r = -0.3663$ and $P < 0.0001$). Unlike RLP-TG, TG did not have a significant correlation with HOMA-R.

To investigate which factors independently determined RLP-TG and TG, we performed multiple regression analysis. Multiple regression analysis with RLP-TG (log) (Table 3(a)) as an objective variable revealed that RBP4 and age had independent relationships with RLP-TG. Multiple regression analysis with TG as an objective variable showed that VFA and age had independent relationships with TG, but RBP4 had no independent relationships with TG (Table 3(b)).

4. Discussion

In the present study, we showed for the first time that serum RBP4 levels correlated with RLP-TG. Univariate analyses showed that RBP4 was significantly associated with RLP-TG and TG. There was no correlation of RBP4 with most of the insulin-resistance-associated factors (adiponectin, VFA, BMI, and HOMA-R) except for a weak correlation with WC, even though most of these factors were significantly correlated with RLP-TG. Furthermore, multiple regression analysis revealed that RBP4 had an independent association with RLP-TG, although RBP4 did not have an independent association with TG levels. These results suggested that RBP4 could regulate TG metabolism especially at the remnant lipoprotein level.

RBP4 was identified as a signal transferring protein for insulin resistance. Therefore, we focused mainly on its relationship with insulin-resistant states in this study, although some reports have shown that RBP4 could play a more important role in lipid metabolism than in insulin resistance [13]. RBP4 correlates with serum TG levels in type 2 diabetic patients independent from liver fat content [14, 15]. Furthermore, some reports have shown that RBP4 correlates with hypertriglyceridemia independent of insulin resistance [4, 13, 16]. In this study, serum RBP4 levels significantly correlated with parameters relating to RLP-TG and TG. Among the generally accepted markers for insulin resistance, no significant relationships were observed between RBP4 and BMI, VFA, HOMA-R, or adiponectin. WC showed a relatively weak relationship with RBP4. The correlation with WC is indirect and is usually considered as a surrogate marker reflecting the extent of insulin resistance. Actually, the appropriate cutoff value of WC to detect metabolic syndrome is still under discussion [17]. However, it is still unclear why RBP4 correlated only with WC instead of VFA which is closely related to insulin resistance. Imbalance of fat distribution in the study group may explain this dissociation. Even under these conditions, RBP4 can regulate TG metabolism especially at the remnant level, but visceral fat accumulation and factors associated with insulin resistance may not be the main pathway for RBP4 to regulate TG metabolism.

Two possible mechanisms explaining the increased level of RLP-TG could be presented, one is the decreased metabolism of TG caused by decreased LPL activity induced by insulin resistance [18] and another is the overproduction of TG. Decreased LPL activity accounts for a great deal of the elevation of serum TG in insulin-deficient diabetes patients [19, 20]. As the RLP-TG to TG ratio has been reported to correlate with LPL activity [21], the result of a significant and positive relationship between RBP4 and the RLP-TG to TG ratio in this study suggests that decreased LPL activity would have contributed much to the elevation of RLP-TG. In addition, RBP4 carries ligands of retinoid X receptor (RXR), and RXR modulates the expression of several genes including apoC-III, which is an inhibitor of the lipoprotein lipase [22, 23]. Based on the present findings and previous reports, RBP4

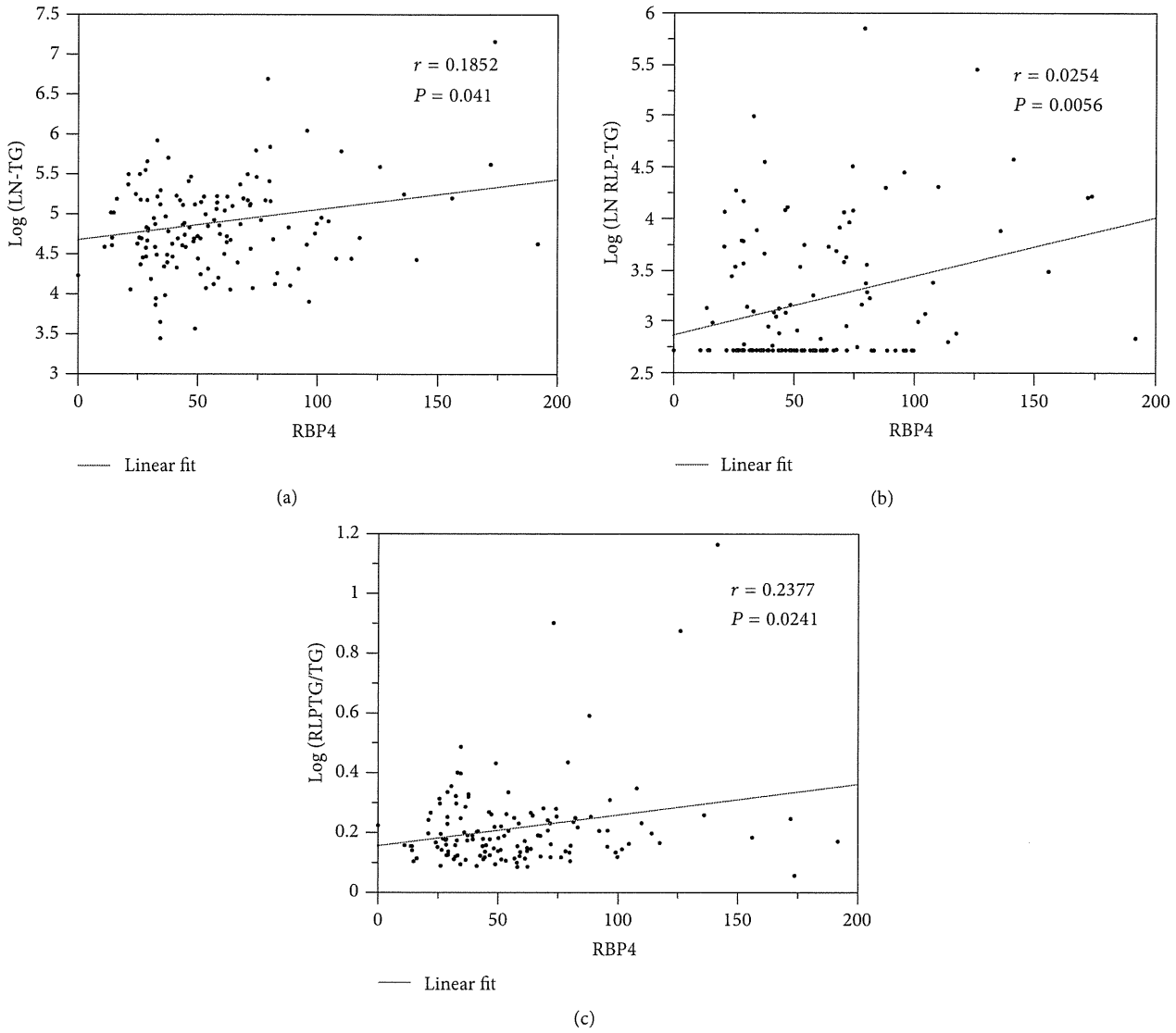

FIGURE 1: Relationship between serum RBP4 levels and logarithm transformed triglyceride (TG) levels (a), logarithm transformed RLP-TG levels (b), and RLP-TG/TG ratio (c).

is thought to increase RLP-TG through the activation of RXR, inducing the overexpression of apoC-III and decreasing LPL activity in type 2 diabetic patients.

This study has several limitations. First, we did not measured LPL activity. As the RLP-TG to TG ratio has been reported to correlate with LPL activity [21], we used a surrogate marker of RLP-TG to TG ratios for LPL activity. Although direct measurement would be ideal, our current results seemed to justify using a surrogate marker to represent LPL activity. Second, some patients were treated with insulin or sulphonylureas, which might affect RBP4 metabolism. However, these medicines were discontinued the day prior to the examination, so the effect on remnant metabolism would be minimized.

In conclusion, RBP4 correlates positively with serum RLP-TG independent of markers reflecting insulin resistance including visceral fat accumulation in patients with type 2 diabetes mellitus. These results suggest that RBP4 may have a negative effect on remnant metabolism independent of visceral fat accumulation, glycemic control, or factors associated with insulin resistance.

References

[1] Q. Yang, T. E. Graham, N. Mody et al., "Serum retinol binding protein 4 contributes to insulin resistance in obesity and type 2 diabetes," *Nature*, vol. 436, no. 7049, pp. 356–362, 2005.

[2] N. Klöting, T. E. Graham, J. Berndt et al., "Serum retinol-binding protein is more highly expressed in visceral than in subcutaneous adipose tissue and is a marker of intra-abdominal fat mass," *Cell Metabolism*, vol. 6, no. 1, pp. 79–87, 2007.

[3] T. E. Graham, Q. Yang, M. Blüher et al., "Retinol-binding protein 4 and insulin resistance in lean, obese, and diabetic subjects," *New England Journal of Medicine*, vol. 354, no. 24, pp. 2552–2563, 2006.

[4] K. Takebayashi, M. Suetsugu, S. Wakabayashi, Y. Aso, and T. Inukai, "Retinol binding protein-4 levels and clinical features of type 2 diabetes patients," *Journal of Clinical Endocrinology and Metabolism*, vol. 92, no. 7, pp. 2712–2719, 2007.

[5] T. Nakamura, J. E. Obata, M. Hirano et al., "Predictive value of remnant lipoprotein for cardiovascular events in patients with coronary artery disease after achievement of LDL-cholesterol goals," *Atherosclerosis*, vol. 218, no. 1, pp. 163–167, 2011.

[6] J. Pang, D. C. Chan, P. H. Barrett, and G. F. Watts, "Postprandial dyslipidaemia and diabetes: mechanistic and therapeutic aspects," *Current Opinion in Lipidology*, vol. 23, no. 4, pp. 303–309, 2012.

[7] M. Ohira, Y. Miyashita, M. Ebisuno et al., "Effect of metformin on serum lipoprotein lipase mass levels and LDL particle size in type 2 diabetes mellitus patients," *Diabetes Research and Clinical Practice*, vol. 78, no. 1, pp. 34–41, 2007.

[8] K. Shirai, Y. Itoh, H. Sasaki et al., "The effect of insulin sensitizer, troglitazone, on lipoprotein lipase mass in preheparin serum," *Diabetes Research and Clinical Practice*, vol. 46, no. 1, pp. 35–41, 1999.

[9] Examination Committee of Criteria for 'Obesity Disease' in Japan and Japan Society for the Study of Obesity, "New criteria for 'obesity disease' in Japan," *Circulation Journal*, vol. 66, no. 11, pp. 987–992, 2002.

[10] R. Kahn, "Report of the expert committee on the diagnosis and classification of diabetes mellitus," *Diabetes Care*, vol. 20, no. 7, pp. 1183–1197, 1997.

[11] T. Yoshizumi, T. Nakamura, M. Yamane et al., "Abdominal fat: standardized technique for measurement at CT," *Radiology*, vol. 211, no. 1, pp. 283–286, 1999.

[12] J. Kobayashi, T. Maruyama, H. Watanabe et al., "Gender differences in the effect of type 2 diabetes on serum lipids, preheparin plasma lipoprotein lipase mass and other metabolic parameters in Japanese population," *Diabetes Research and Clinical Practice*, vol. 62, no. 1, pp. 39–45, 2003.

[13] M. von Eynatten, P. M. Lepper, D. Liu et al., "Retinol-binding protein 4 is associated with components of the metabolic syndrome, but not with insulin resistance, in men with type 2 diabetes or coronary artery disease," *Diabetologia*, vol. 50, no. 9, pp. 1930–1937, 2007.

[14] B. Verges, B. Guiu, J. P. Cercueil et al., "Retinol-binding protein 4 is an independent factor associated with triglycerides and a determinant of very low-density lipoprotein-apolipoprotein b100 catabolism in type 2 diabetes mellitus," *Arteriosclerosis, Thrombosis, and Vascular Biology*, vol. 32, no. 12, pp. 3050–3057, 2012.

[15] S. C. Huang and Y. J. Yang, "Serum retinol-binding protein 4 is independently associated with pediatric NAFLD and fasting triglyceride level," *Journal of Pediatric Gastroenterology and Nutrition*, vol. 56, no. 2, pp. 145–150, 2013.

[16] Q. Qi, Z. Yu, X. Ye et al., "Elevated retinol-binding protein 4 levels are associated with metabolic syndrome in Chinese people," *Journal of Clinical Endocrinology and Metabolism*, vol. 92, no. 12, pp. 4827–4834, 2007.

[17] R. Oka, J. Kobayashi, K. Yagi et al., "Reassessment of the cutoff values of waist circumference and visceral fat area for identifying Japanese subjects at risk for the metabolic syndrome," *Diabetes Research and Clinical Practice*, vol. 79, no. 3, pp. 474–481, 2008.

[18] J. Kobayashi, K. Saito, I. Fukamachi et al., "Pre-heparin plasma lipoprotein lipase mass: correlation with intra-abdominal visceral fat accumulation," *Hormone and Metabolic Research*, vol. 33, no. 7, pp. 412–416, 2001.

[19] E. A. Nikkila, J. K. Huttunen, and C. Ehnholm, "Postheparin plasma lipoprotein lipase and hepatic lipase in diabetes mellitus. Relationship to plasma triglyceride metabolism," *Diabetes*, vol. 26, no. 1, pp. 11–21, 1977.

[20] J. Kobayashi, K. Nakajima, A. Nohara et al., "The relationship of serum lipoprotein lipase mass with fasting serum apolipoprotein B-48 and remnant-like particle triglycerides in type 2 diabetic patients," *Hormone and Metabolic Research*, vol. 39, no. 8, pp. 612–616, 2007.

[21] T. Nakano, Y. Tokita, T. Nagamine et al., "Measurement of serum remnant-like lipoprotein particle-triglyceride (RLP-TG) and RLP-TG/total TG ratio using highly sensitive triglyceride assay reagent," *Clinica Chimica Acta*, vol. 412, no. 1-2, pp. 71–78, 2011.

[22] N. Noy, "Retinoid-binding proteins: mediators of retinoid action," *Biochemical Journal*, vol. 348, no. 3, pp. 481–495, 2000.

[23] N. Vu-Dac, P. Gervois, I. P. Torra et al., "Retinoids increase human apo C-III expression at the transcriptional level via the retinoid X receptor: contribution to the hypertriglyceridemic action of retinoids," *Journal of Clinical Investigation*, vol. 102, no. 3, pp. 625–632, 1998.

TFE3 Controls Lipid Metabolism in Adipose Tissue of Male Mice by Suppressing Lipolysis and Thermogenesis

Yuri Fujimoto,* Yoshimi Nakagawa,* Aoi Satoh,* Kanako Okuda, Akiko Shingyouchi, Ayano Naka, Takashi Matsuzaka, Hitoshi Iwasaki, Kazuto Kobayashi, Naoya Yahagi, Masako Shimada, Shigeru Yatoh, Hiroaki Suzuki, Satomi Yogosawa, Tetsuro Izumi, Hirohito Sone, Osamu Urayama, Nobuhiro Yamada, and Hitoshi Shimano

Department of Internal Medicine (Metabolism and Endocrinology) (Y.F., Y.N., A.Sa., K.O., A.Sh., A.N., T.M., H.I., K.K., N.Yah., M.S., S.Ya., H.Su., H.So., O.U., N.Yam., H.Sh.), Faculty of Medicine, University of Tsukuba, Tsukuba, Japan 305–8575; Laboratory of Molecular Endocrinology and Metabolism (S.Yo., T.I.), Department of Molecular Medicine, Institute for Molecular and Cellular Regulation, Gunma University, Maebashi, Japan 371–8512; and International Institute for Integrative Sleep Medicine (H.Sh.), University of Tsukuba, Tsukuba, Japan 305–8575

Transcription factor E3 (TFE3) is a transcription factor that binds to E-box motifs and promotes energy metabolism-related genes. We previously reported that TFE3 directly binds to the insulin receptor substrate-2 promoter in the liver, resulting in increased insulin response. However, the role of TFE3 in other tissues remains unclear. In this study, we generated adipose-specific TFE3 transgenic (aP2-TFE3 Tg) mice. These mice had a higher weight of white adipose tissue (WAT) and brown adipose tissue than wild-type (WT) mice under fasting conditions. Lipase activity in the WAT in these mice was lower than that in the WT mice. The mRNA level of adipose triglyceride lipase (ATGL), the rate-limiting enzyme for adipocyte lipolysis, was significantly decreased in aP2-TFE3 Tg mice. The expression of Foxo1, which directly activates ATGL expression, was also suppressed in transgenic mice. Promoter analysis confirmed that TFE3 suppressed promoter activities of the *ATGL* gene. In contrast, G0S2 and Perilipin1, which attenuate ATGL activity, were higher in transgenic mice than in WT mice. These results indicated that the decrease in lipase activity in adipose tissues was due to a decrease in ATGL expression and suppression of ATGL activity. We also showed that thermogenesis was suppressed in aP2-TFE3 Tg mice. The decrease in lipolysis in WAT of aP2-TFE3 Tg mice inhibited the supply of fatty acids to brown adipose tissue, resulting in the inhibition of the expression of thermogenesis-related genes such as *UCP1*. Our data provide new evidence that TFE3 regulates lipid metabolism by controlling the gene expression related to lipolysis and thermogenesis in adipose tissue. **(*Endocrinology* 154: 3577–3588, 2013)**

Adipose tissue plays a critical role in regulating energy balance. In addition to being a reserve of fuel in mammals, white adipose tissue (WAT) plays an important role in lipid metabolism, including the storage of triacylglycerol (TAG) for lipolysis to provide fatty acids (FAs) as an energy source for other organs. Brown adipose tissue (BAT) functions in thermogenesis using FAs produced from lipolysis in WAT to activate uncoupling protein (UCP) 1 and mitochondrial β-oxidation (1).

Three enzymes are involved in the complete hydrolysis of TAG molecules in cellular lipid stores. The first and rate-limiting step hydrolyzes TAGs to generate diacylglycerols and nonesterified fatty acids, which are then cat-

ISSN Print 0013-7227 ISSN Online 1945-7170
Printed in U.S.A.

Received March 1, 2013. Accepted July 16, 2013.
First Published Online July 24, 2013

* Y.F., Y.N., and A.Sa. contributed equally to this work.

Abbreviations: ADRP/ADFP, adipose differentiation-related protein; aP2, fatty acid-binding protein 4; aP2-TFE3 Tg, adipose-specific TFE3 transgenic; ATGL, adipose triglyceride lipase; ATGL KO, ATGL deficient; BAT, brown adipose tissue; C/EBP, CCAAT/enhancer-binding protein; CGI-58, comparative gene identification-58; FA, fatty acid; FAS, fatty acid synthase; FBS, fetal bovine serum; FFA, free fatty acid; Foxo, Forkhead box O; G0S2, G0/G1 switch 2; HA, hemagglutinin; HEK, human embryonic kidney; HFHS, high-fat, high-sucrose; HSL, hormone-sensitive lipase; IRF4, interferon regulatory factor 4; IRS, insulin receptor substrate; PGC-1α, PPAR, peroxisome proliferative-activated receptor, gamma, coactivator 1 alpha; Q-PCR, quantitative PCR; RNAi, RNA interference; RT, room temperature; TAG, triacylglycerol; TFE3, transcription factor E3; UCP, uncoupling protein; WAT, white adipose tissue; WT, wild type.

alyzed by adipose triglyceride lipase (ATGL). The next step is catalyzed by hormone-sensitive lipase (HSL), a multifunctional enzyme that hydrolyzes various acyl esters, including TAG, diacylglycerols, and monoacylglycerol. The last step involves monoglyceride lipase, which cleaves monoacylglycerol into glycerol and nonesterified fatty acids (2).

The physiological functions of ATGL have been investigated in whole-body and adipose-specific knockout (KO) mouse models (3–5). The whole-body ATGL-deficient (ATGL KO) mouse has increased adipose mass and develops TAG deposition in multiple tissues. The mice also accumulate large amounts of lipid in the heart, which causes cardiac dysfunction and premature death (5). The decreased availability of ATGL-derived free fatty acids (FFAs) leads to increases in glucose use and tolerance and increased insulin sensitivity (5). It was recently reported that adipose-specific ATGL-deficient mice possessed adipose lipolysis that was crucial for fasting energy homeostasis (4) and had markedly deficient lipolysis in the fasted state. These mice also had a mild increase in the body fat content, insulin sensitivity, and light-phase hyperphagia. A supply of FAs from lipolysis is critical for β-oxidation and UCP1 activation for thermogenesis. ATGL KO mice therefore have impaired thermogenesis because of decreased UCP1 expression with lower peroxisome proliferator-activated receptor (PPAR)-α binding to its promoter and subsequent activation (3).

The leucine zipper-containing basic helix loop helix protein transcription factor E3 (TFE3) was originally identified as a transcription factor involved in regulation of the expression of the gene encoding the immunoglobulin heavy chain by binding to the intron enhancer (6). The *TFE* gene family has also been shown to be involved in the biology of melanocytes and development of their malignancies. In addition to functioning as homodimers, TFEs work as partners of other transcriptional regulators such as E2F, PU.1, Max, and Smads in the regulation of various genes (7–9). Moreover, at least 5 different translocations involving the Xp11.2 chromosomal region reportedly fuse with TFE3 and are predicted to produce ASPL-TFE3, PRCC-TFE3, NonO-TFE3, CLTC-TFE3, and protein-associated splicing factor-TFE3 fusion proteins (10). The involvement of TFE3 in these 5 different gene fusions in renal cell carcinomas is consistent with a central role for TFE3-related transcriptional deregulation in these tumors. TFE3 acts as a rheostat for controlled disequilibration of the regulatory network that establishes ground-state pluripotency in the embryo, thereby sustaining embryonic stem cells (11).

In the immune system, TFE3 plays an important regulatory role in B and T cells. TFE3 and TFEB, one of the TFE3 family molecules, are the direct activators of CD40 ligand expression in activated CD4+ T cells critical for T cell-dependent antibody responses (12). Recently we showed that this transcriptional factor is involved in hepatic glucose metabolism (13). In primary hepatocytes and the mouse liver, in which TFE3 was overexpressed, we observed a significant up-regulation in gene expression of insulin receptor substrate (IRS)-2, Akt/protein kinase B, and hexokinase 2, all of which are involved in insulin signaling or its action. In addition, increased levels of the IRS-2 protein were associated with enhanced phosphorylation of Akt and glycogen synthase kinase-3 and concomitant activation of glycogen synthesis. These changes decreased hyperglycemia in both normal and diabetic mice by enhancing insulin signaling (13). In muscle-specific TFE3 transgenic mice, muscle glycogen stores increased in accordance with regulation of the expression of genes involved in glucose metabolism. Consequently, these mice have high exercise endurance capacity, and after exercise training, they have a greater insulin response than wild-type (WT) mice (14).

However, the functions of TFE3 in adipose tissue remain unclear. In this study, we generated adipose-specific TFE3 transgenic (aP2-TFE3 Tg) mice to investigate the effects of TFE3 on lipid metabolism in adipose tissues.

Materials and Methods

Generation of transgenic mice

A chimeric gene was constructed that included 5.4 kb of the mouse fatty acid-binding protein 4 (aP2) gene promoter linked to 1.7 kb of mouse TFE3 cDNA (NM_172472) with an hemagglutinin (HA) tag in the N terminus, followed by a polyadenylation signal from the human GH gene. The cDNA of mouse TFE3 was obtained by PCR, as described previously. Constructed transgene fragments were inserted by microinjection into C57BL/6J mouse eggs at the Laboratory Animal Resource Center (University of Tsukuba). We used male mice in all experiments. The mice were maintained on a fixed light/dark cycle and fed a regular chow diet (MF; Oriental Yeast, Tokyo, Japan). All the experiments were performed according to the Guide for the Care and Use of Laboratory Animals of the University of Tsukuba and were approved by the institutional review board.

Western blotting

Total cell lysates were prepared from tissues as described previously (13). Anti-TFE3 antibody was purchased from BD Biosciences (Franklin Lakes, New Jersey), anti-α-tubulin antibody from Calbiochem (La Jolla, California), and antiphospho-Akt (Ser473) and Akt antibodies from Cell Signaling Technology (Beverly, Massachusetts). The blots were visualized by Chemi-Doc XRS+ (Bio-Rad Laboratories, Hercules California) and quantified by Image Lab Software (Bio-Rad Laboratories).

Metabolic measurements

The plasma levels of glucose, insulin, triglycerides, FFAs, and cholesterol were measured as described previously (13).

Histological analysis

WAT was fixed, embedded in paraffin, sectioned, and stained with hematoxylin and eosin. Adipocyte cell size was determined by Image J software (National Institutes of Health, Bethesda, Maryland), with the measurement of at least 300 cells in each sample.

Primary adipocyte cell isolation and culture

Mouse primary adipocytes from WAT were isolated using a modification of the method of Ahmadian et al (3). In brief, WAT was digested for 1 hour at 37°C with collagenase (type II; Sigma, St Louis, Missouri) in Krebs-Ringer buffer (12 mM HEPES, 121 mM NaCl, 4.9 mM KCl, 1.2 mM $MgSO_4$, and 0.33 mM $CaCl_2$) supplemented with 0.1% glucose and 1% FA-free BSA, filtered through nylon mesh, and centrifuged, after which adipocytes were collected from the upper phase. The pellet containing the stromal vascular fraction was filtered through a 40-μm cell strainer and centrifuged. Primary adipocytes were cultured in MEMα (Invitrogen) supplemented with 10% fetal bovine serum (FBS) and penicillin-streptomycin. The mouse primary adipocytes were then induced to differentiate into mature adipocytes (15), and after 8 days the cells were stained with Oil Red-O, followed by extraction of the absorbed stain using 100% isopropanol and measurement at 490 nm, as described previously (16).

Analysis of gene expression

Total RNA from the cells and tissues was prepared using Sepasol-RNA I (Nacalai Tesque, Kyoto, Japan). For real-time PCR analysis, total RNA was used for cDNA synthesis (Invitrogen, Carlsbad, California). Real-time PCR was performed using the ABI Prism 7300 System (Applied Biosystems Inc, Foster City, California) with SYBR Green master mix (Roche, Stockholm, Sweden). The primer sequences are shown in Supplemental Table 1, published on The Endocrine Society's Journals Online web site at http://endo.endojournals.org. Gene expression was normalized to cyclophilin expression, with the data analyzed using the comparative cycle threshold method.

Adipocyte isolation and in vitro lipolysis

Adipocytes were isolated from the WAT of 8-week-old male WT mice and aP2-TFE3 Tg mice as described by Yang et al (17). Lipolysis was measured in the presence of 10 μM isoproterenol for the times indicated.

In vivo lipolysis assay

Eight-week-old male mice were fasted for 24 hours and then ip injected with isoproterenol (10 mg/kg body weight). Blood was collected from the mice before and 2 hours after the injection. The levels of glycerol and FFAs in plasma were determined as described previously (17).

Plasmid constructs

The expression plasmids TFE3 and Forkhead box O (Foxo)-1 3A (dominant active form of Foxo1; (NM_019739) were constructed as described previously (13, 18). The ATGL promoter (base pairs −3979 to +81) was subcloned into the pGL4.10 luciferase vector (Promega, Madison, Wisconsin) as described previously (19).

Luciferase analysis

Human embryonic kidney (HEK)-293 cells were grown at 37°C in an atmosphere of 5% CO_2 in DMEM (Invitrogen) supplemented with 10% FBS and penicillin-streptomycin. Before transfection, the HEK293 cells were seeded in 24-well plates at a density of 2.5×10^4 cells/well. After adhesion, the cells were transfected with FuGENE 6 (Roche) according to the manufacturer's protocol. The total amount of DNA was adjusted to 0.3 μg/well in 24-well plates with empty vector DNA. After 24 hours of transfection, the cells were washed with PBS and harvested. Luciferase assays were performed according to the manufacturer's protocol using the dual-luciferase assay kit (Promega), with luciferase activity being quantified by a Wallac 1420 multilabel counter (PerkinElmer Life Sciences, Boston, Massachusetts). The internal standard, Simian virus 40 Renilla luciferase control vector, was also cotransfected to normalize for transfection efficiency.

3T3-L1 cell culture, adipocyte differentiation, and adenovirus infection

3T3-L1 cells were maintained in DMEM (Invitrogen) supplemented with 10% FBS and penicillin-streptomycin. The cells were cultured to confluence. 3T3-L1 adipocytes were infected with adenoviruses (1000 OPU/cell) encoding LacZ RNA interference [(RNAi); LacZi] or TFE3 RNAi (TFE3i), followed by incubation for 2 days.

Statistical analyses

Statistical significance was calculated by unpaired Student's t tests, with $P < .05$ considered significant. All data were expressed as the mean ± SEM.

Results

The expression pattern of TFE3 mRNA in adipose tissues

We reported previously that the expression of TFE3 in mice was high in tissues involved in energy metabolism such as the liver and WAT (13). In this study, we focused on the roles of TFE3 in adipose tissues. First, we checked whether the expression of TFE3 mRNA was nutritionally regulated using quantitative PCR (Q-PCR) analysis to evaluate the level of expression in different nutritional states. The expression levels of TFE3 mRNA in WAT of WT mice were higher in the refed condition than in the fasted condition (Figure 1A). The levels of TFE3 mRNA from *ob/ob* (leptin deficient) mice were significantly higher than those in the WT mice in both the fasted and refed conditions (Figure 1A). In addition, the expression levels of TFE3 mRNA in WAT of mice fed a high-fat,

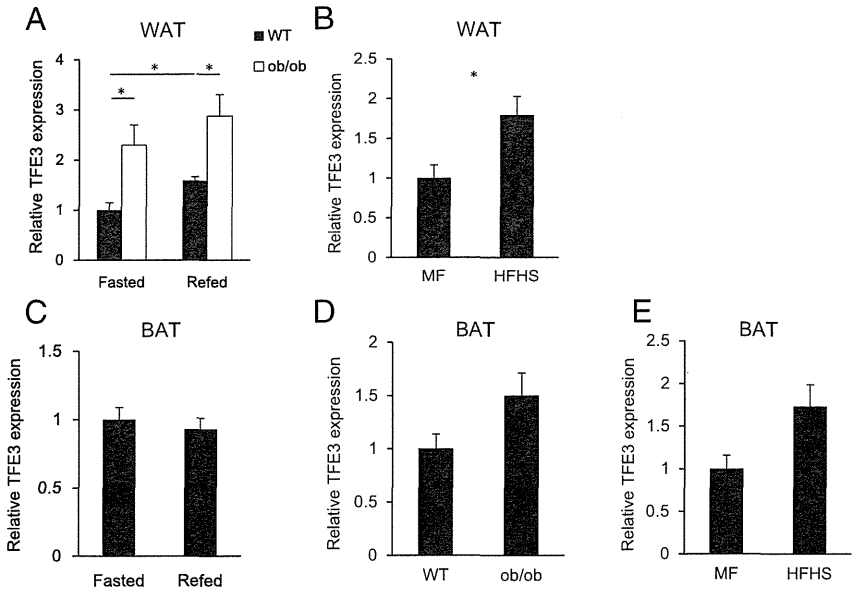

Figure 1. Expression of TFE3 was increased in WAT and BAT during excess nutrient intake. A, TFE3 mRNA from WAT of 8-week-old male WT and leptin-deficient (*ob/ob*) mice in the fasted and refed states, estimated by Q-PCR. B, TFE3 mRNA from WAT of 4-week-old male WT mice fed a normal diet (MF) or a HFHS diet for 8 weeks. C–E, TFE3 mRNA from BAT of 8-week-old male WT in the fasted and refed states (C), 8-week-old male WT, and *ob/ob* fed ad libitum (D), and 4-week-old male WT mice fed a MF or an HFHS diet for 8 weeks (E). The results are expressed as means ± SEM. *, $P < .05$, **, $P < .01$ vs WT mice or fed a MF.

high-sucrose (HFHS) diet were up-regulated compared with those in WT mice (Figure 1B). However, there were no apparent differences in the expression levels in the BAT between the fasted and refed conditions (Figure 1C). Levels of TFE3 mRNA in the BAT of *ob/ob* mice and HFHS-fed mice tended to be increased compared with those in WT mice (Figure 1, D and E). These results suggested that TFE3 mRNA is nutritionally regulated in WAT and that TFE3 may play an important role in lipid metabolism and the development of obesity.

Generation of aP2-TFE3 Tg mice

To investigate the roles of TFE3 in adipose tissues, we generated aP2-TFE3 Tg mice using an HA-tagged TFE3 cDNA and an adipose tissue specific promoter/enhancer region of the mouse *aP2* gene, which is also called fatty acid-binding protein 4 (Figure 2A). Although aP2 was originally identified as an adipocyte-specific protein, recent studies have shown that aP2 is also expressed in other tissues, including the brain, heart, kidney, spleen, muscle, macrophages, lymphatic system, and skin and during embryogenesis (20–27).

To confirm the expression of the transgene, we measured TFE3 expression in various tissues using Northern blot and Q-PCR. Transgenic expression of TFE3 mRNA was mainly detected in the WAT and BAT using Northern blot analysis, with the expression being apparently higher in the BAT (Figure 2B). Moreover, Q-PCR analysis revealed that the increase in TFE3 expression was obtained in other tissues, including the brain, heart, kidney, spleen, skeletal muscle, and skin (Figure 2C). The increase in TFE3 mRNA was observed in both adipocyte and stromal vascular fraction isolated from WAT (Figure 2C). We also confirmed the TFE3 protein from the transgene in WAT and BAT by Western blotting. The ectopic TFE3 protein was detected at higher levels in the BAT than in WAT, a finding consistent with the levels of TFE3 transgene (Figure 2D). Although Figure 2D shows 2 different sizes of TFE3 proteins, these proteins had similar transcriptional activity as reported previously (13). Histological analysis and cell size measurement revealed that the adipocytes in epididymal WAT from the aP2-TFE3 Tg mice under fasting conditions tended to be slightly larger than those from the WT mice (Figure 2, E and F). However, these differences were not significantly different.

The phenotypes of the aP2-TFE3 Tg mice

We investigated the differences between the WT and aP2-TFE3 Tg mice under fasting conditions. At 8 weeks of age, body weight and liver weight were not different between the 2 groups of mice, whereas the weight of WAT and BAT were significant higher in the aP2-TFE3 Tg mice than in the WT mice. Plasma triglyceride contents in the aP2-TFE3 Tg mice during fasting were significantly higher than those in the WT mice, whereas plasma glucose, insulin, and cholesterol levels were similar (Table 1). The levels of plasma FFAs in the aP2-TFE3 Tg mice were marginally higher under fasting conditions, although this difference was not statistically significant (Table 1). The levels of metabolic parameters were not significantly different between the 2 groups of mice under ad libitum conditions (Table 1). These findings indicate that there are differences in lipid metabolism between the WT and aP2-TFE3 Tg mice under fasting conditions.

Dysregulation of lipolysis in WAT in aP2-TFE3 Tg mice

Adipose tissue triglyceride metabolism was investigated in the aP2-TFE3 Tg mice based on the difference in plasma triglyceride levels. To study the direct effects of

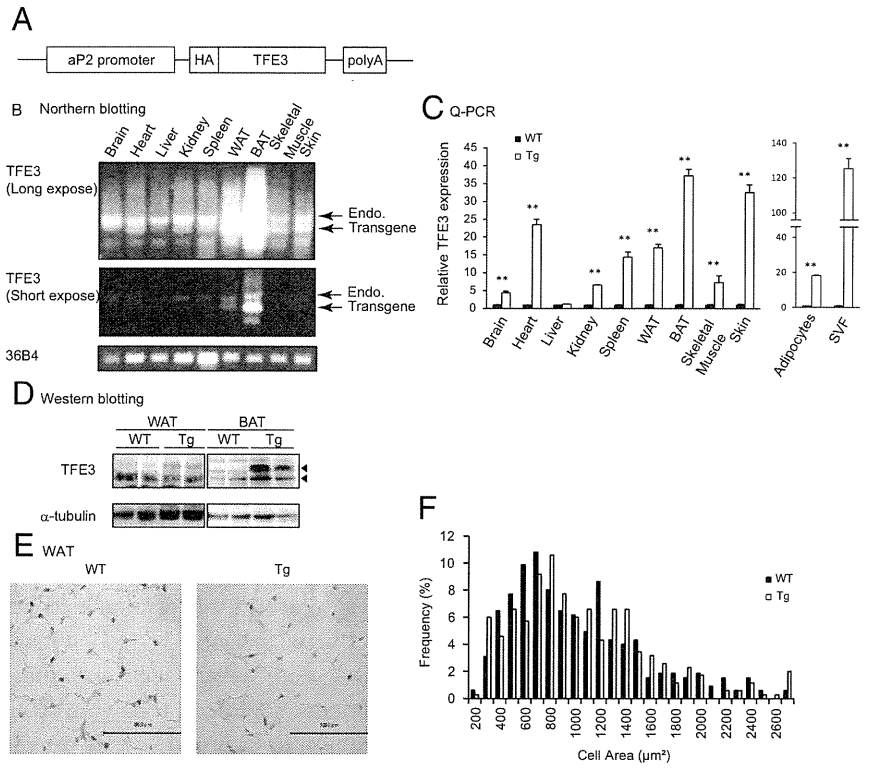

Figure 2. Generation of adipocyte-specific TFE3 overexpression in transgenic mice (aP2-TFE3 Tg mice). A, Schematic diagram of the aP2-TFE3 Tg mice. A chimeric gene was constructed and included 5.4 kb of the mouse fatty acid-binding protein 4 (aP2) gene promoter linked to 1.7 kb of mouse TFE3 cDNA with an HA tag in the N terminus, followed by a polyadenylation signal from the *hGH* gene. B, The tissue distribution of endogenous (Endo) and transgene TFE3 (Transgene) mRNA was determined by Northern blotting, with 36B4 being used as the standard. C, TFE3 mRNA in various tissues from 12-week-old male WT and aP2-TFE3 Tg mice was determined by Q-PCR (n = 3). D, TFE3 protein levels were estimated in WAT and BAT of the male WT and aP2-TFE3 Tg mice by Western blotting, with α-tubulin being used as the standard. E, Hematoxylin and eosin staining of paraffin-embedded WAT sections from 12-week-old male WT and aP2-TFE3 Tg mice after a 24-hour fast. The scale bars represent 100 μm. F, Histogram of adipocyte size in WAT from 12-week-old male WT and aP2-TFE3 Tg mice (n = 3). The results are expressed as means ± SEM. *, $P < .05$, **, $P < .01$ vs WT mice.

TFE3 on lipid metabolism, we measured lipolysis activity in WAT by isolating adipocytes from the WT and aP2-TFE3 Tg mice and measuring the release of glycerol and FFAs from these cells for 2 hours after treatment with isoproterenol, which stimulates lipolysis by increasing cellular cAMP levels. Under basal conditions, the rates of glycerol and FFA release were similar in isolated adipocytes from both the WT and aP2-TFE3 Tg mice. Under isoproterenol-stimulated (stimulated) conditions, lipolysis was induced in adipocytes from both mice. However, compared with the WT mice, glycerol and FFA release were significantly lower in isolated adipocytes from the aP2-TFE3 Tg mice (Figure 3A). To further investigate lipolysis activity, the mice were iv injected with isoproterenol in the fasted condition, and plasma glycerol and FFA concentrations measured before (pre) and 2 hours after (post) the injection. Under basal conditions (pre), the amount of glycerol and FFAs released was not different in the WT and aP2-TFE3 Tg mice. However, the levels of plasma FFAs in the aP2-TFE3 Tg mice after the injection of isoproterenol were lower than those in the WT mice, whereas the levels of plasma glycerol remained unchanged (Figure 3B). These results suggested that lipolysis activity of WAT was suppressed in the aP2-TFE3 Tg mice.

Gene expression in WAT of aP2-TFE3 Tg mice

Because the aP2-TFE3 Tg mice had defects in lipolysis in WAT, we hypothesized that TFE3 may suppress the expression of lipases, including ATGL and HSL, in these mice. We determined gene expression related to lipolysis in WAT of the WT and aP2-TFE3 Tg mice using Q-PCR. In the fasted state, ATGL mRNA in WAT in the aP2-TFE3 Tg mice was significantly down-regulated compared with that in the WT mice (Figure 4A). Previous studies (3, 28) showed ATGL expression was regulated by Foxo1 and interferon regulatory factor 4 (IRF4). Foxo1 mRNA in WAT from the aP2-TFE3 Tg mice was down-regulated significantly compared with that in WAT from the WT mice. The expression of IRF4 mRNA also tended to be reduced in the aP2-TFE3 Tg mice compared with that in the WT mice, although this difference was not statistically significant.

In addition, mRNA levels of Perilipin1 and G0/G1 switch 2 (G0S2), which inactivate ATGL enzymatic activity, were up-regulated in the aP2-TFE3 Tg mice. The expression of comparative gene identification-58 (CGI-58), which activates lipolysis, did not differ in the 2 strains of mice. Taken together, these results suggest that the suppression of lipolysis in the aP2-TFE3 Tg mice depends on the suppression of both ATGL expression and its enzymatic activation. As shown in Figure 4B, thermogenesis genes such as UCP1 and UCP2 were reduced significantly in the aP2-TFE3 Tg mice, whereas UCP3 and PPARα remained unchanged in both strains of mice. Peroxisome proliferative-activated receptor gamma coactivator 1 alpha (PGC-1α) mRNA tended to decrease in the aP2-TFE3 Tg mice, although this change was not statistically signif-

Table 1. Metabolic Parameters in 8-Week-Old Male Mice in 24 Hour-Fasted and Fed ad Libitum Conditions

	Fasted			Fed		
	WT	Tg		WT	Tg	*P* Value
Body weight, g	22.4 ± 0.4	21.2 ± 0.36	ns	23.3 ± 0.37	22.51 ± 0.37	ns
Liver weight, g	0.828 ± 0.02	0.818 ± 0.03	ns	1.059 ± 0.02	1.047 ± 0.004	ns
WAT weight, g	0.234 ± 0.03	0.29 ± 0.02	$P < .05$	0.298 ± 0.012	0.336 ± 0.023	ns
BAT weight, g	0.047 ± 0.006	0.066 ± 0.004	$P < .01$	0.069 ± 0.004	0.07 ± 0.004	ns
Plasma glucose, mg/dL	93.2 ± 3.2	102.6 ± 5.3	ns	179.9 ± 6.4	186.5 ± 10.2	ns
Plasma insulin, pg/mL	481.2 ± 128.2	373.7 ± 206.1	ns	862.1 ± 131.5	864.7 ± 55.5	ns
Plasma TG, mg/dL	99.4 ± 12.2	149.9 ± 14.6	$P < .05$	85.2 ± 8.6	80.8 ± 4.8	ns
Plasma TC, mg/dL	73.4 ± 4.2	76.4 ± 6.1	ns	67.2 ± 3.8	75 ± 5.6	ns
Plasma FFAs, mEq/L	0.73 ± 0.05	0.81 ± 0.1	ns	0.45 ± 0.02	0.429 ± 0.04	ns

Abbreviations: ns, not significant; TC, total cholesterol; TG, triglyceride; Tg, aP2-TFE3 transgenic mice. Data represent means ± SEM: n = 4–11 in each group.

icant. We next checked the expression of adipogenic and lipogenic genes in WAT in the fasted state, including PPARγ, fatty acid synthase (FAS), CCAAT/enhancer-binding protein-α (C/EBP)-α, C/EBPβ, diacylglycerol O-acyltransferase-1, and adipose differentiation-related protein (ADFP; also known as ADRP). There were no significant differences in the expression levels of FAS, C/EBPβ, and diacylglycerol O-acyltransferase-1 between the WT and aP2-TFE3 Tg mice (Figure 4C). However, the levels of PPARγ and C/EBPα mRNA tended to increase in the aP2-TFE3 Tg mice, whereas those of ADFP tended to decrease, although not significantly (Figure 4C).

We also investigated whether there were differences in adipocyte differentiation using primary adipocytes isolated from the mice. After undergoing differentiation into mature adipocytes, we stained the cells with Oil Red-O to confirm the accumulation of triglyceride and adipose differentiation. We observed no apparent morphological differences in adipocyte differentiation between the WT and aP2-TFE3 Tg mice (Figure 4D, left panel). Quantification of Oil Red-O staining in those cells revealed that the accumulation of triglycerides was not different between the WT and aP2-TFE3 Tg mice (Figure 4D, right panel). However, expression of the PPARγ and ADFP genes was significantly increased in isolated adipocytes from the aP2-TFE3 Tg mice, whereas the expression of the other genes was not different (Figure 4E). These results

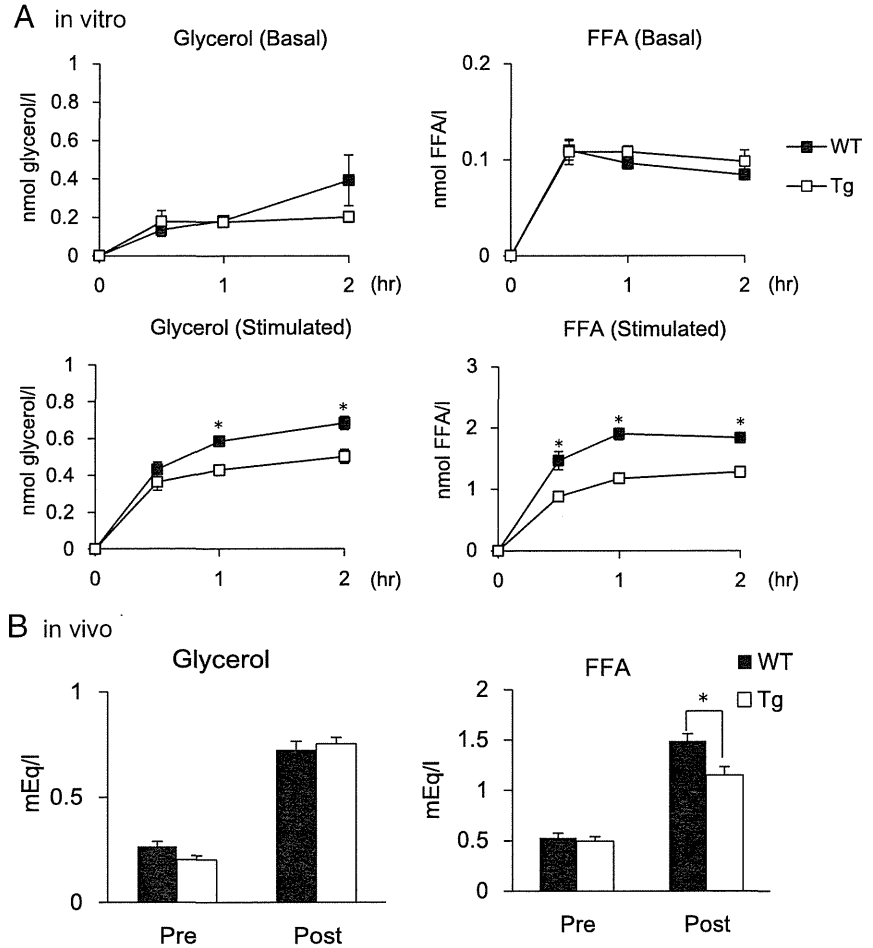

Figure 3. TFE3-attenuated lipolysis in vitro and in vivo. A, The rate of lipolysis in isolated adipocytes from epidermal fat of 12-week-old male WT and aP2-TFE3 Tg mice. The concentrations of glycerol and FFAs released into the media over 2 hours were measured in the presence and absence of 20 μM isoproterenol. The results are expressed as means ± SEM. *, $P < .05$ vs WT mice (n = 5–8). B, Plasma glycerol and FFA concentrations in the male WT and aP2-TFE3 Tg mice measured in the presence (post) and absence (pre) of 10 mg/kg isoproterenol for 2 hours (post) (n = 5–8). The results are expressed as means ± SEM. *, $P < .05$ vs WT mice.

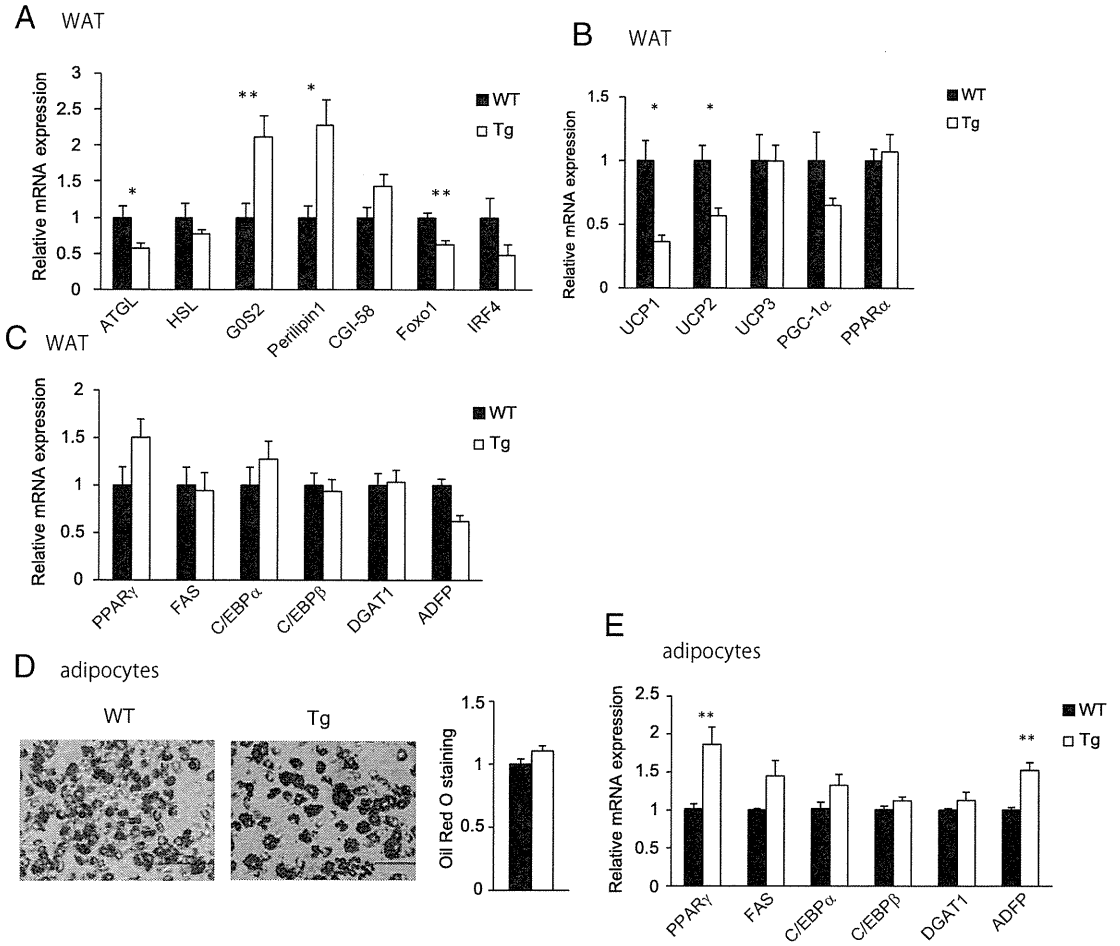

Figure 4. Gene expression in WAT of aP2-TFE3 Tg mice. The expression of lipolysis- (A), thermogenic- (B), and adipogenesis (C)-related genes in WAT in 8-week-old male WT and aP2-TFE3 Tg mice in the fasted state, determined by Q-PCR (n = 6–8). D, The adipocytes were isolated from epidermal fat of 12-week-old male WT and aP2-TFE3 Tg mice. Oil Red-O staining of cells was performed 8 days after the induction of adipocyte differentiation. Quantification of Oil Red-O staining was measured (n = 7). E, Expression of adipogenesis-related genes in adipocytes from 12-week-old male WT and aP2-TFE3 Tg mice 8 days after the induction of adipocyte differentiation (n = 7). The results are expressed as means ± SEM. *, $P < .05$ vs WT mice; **, $P < 0.01$.

indicated that TFE3 suppressed lipolysis, whereas the effects of TFE3 on adipogenesis and lipogenesis in WAT were restrictive.

TFE3 has no effect of insulin signaling in WAT in the fasted condition

Insulin inhibits the expression of ATGL in adipocytes by restraining the nuclear localization of Foxo1; therefore, insulin signaling is important for regulating the expression of ATGL (29). We previously reported that TFE3 up-regulated the expression of IRS-2 and activated insulin signaling in the liver from mice overexpressing TFE3 (13). We determined the expression of IRS-2 and phosphorylated Akt level in WAT from the aP2-TFE3 Tg mice. The expression of IRS-2 tended to be lower in the aP2-TFE3 Tg mice than in the WT mice, although this difference was not significant (Figure 5A). Akt is the downstream protein of IRS-2 and is phosphorylated in response to insulin. The levels of phosphorylated Akt protein were similar in WAT from both the WT and aP2-TFE3 Tg mice (Figure 5B). These findings indicated that TFE3 did not affect insulin signaling in WAT under fasting conditions.

TFE3 suppresses ATGL promoter activity

As shown in Figure 4A, the gene expression of ATGL was significantly lower in the aP2-TFE3 Tg mice than in the WT mice. To investigate the role of TFE3 as a regulator of ATGL promoter activity, we tested whether TFE3 affected the ATGL promoter in HEK293 cells using a luciferase reporter gene linked to the mouse ATGL promoter. The transfection of TFE3 suppressed basal ATGL promoter activity, indicating that TFE3 represses ATGL at the transcriptional level (Figure 6A). A previous report showed that Foxo1 directly bound to the promoter region of ATGL via the insulin response element sequence (29). Using the active mutant of Foxo1, Foxo1 3A, we con-

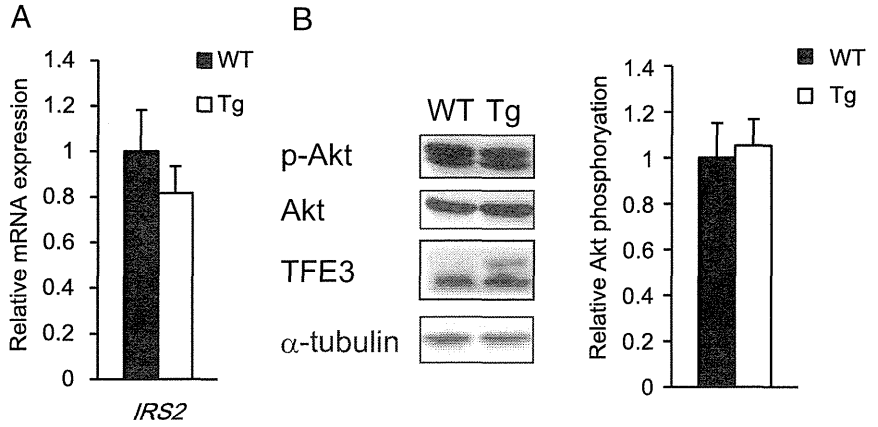

Figure 5. TFE3 had no effects on insulin signaling. A, Gene expression of IRS-2 in WAT from 8-week-old male WT and aP2-TFE3 Tg mice in the fasted state, determined by Q-PCR (n = 3). B, The protein levels of phosphorylated Akt and total Akt contents are shown (left panel). The ratio between phosphorylated Akt and total Akt levels was quantified in WAT (right panel) (n = 3). The results are expressed as means ± SEM.

firmed there was a relationship between TFE3 and Foxo1. Foxo1 3A has 3 Akt-mediated serine-phosphorylation sites, which substitute for alanine, and it is resistant to nuclear exclusion by Akt and is therefore constitutively active (18). Foxo1-mediated activation of the ATGL promoter was enhanced by this mutation but was still completely suppressed by the coexpression of TFE3 (Figure 6A). As shown in Figure 6B, ATGL promoter activity induced by Foxo1 3A was repressed by TFE3 in a dose-dependent manner. To confirm the results of luciferase analysis, we next performed knockdown analysis for TFE3 in 3T3-L1 preadipocytes. When 3T3-L1 adipocytes were infected with adenoviruses encoding short hairpin RNA against TFE3 (TFE3i), TFE3i significantly activated ATGL expression compared with LacZi (Figure 6C). These findings raised the possibility that the inhibitory action of TFE3 on ATGL expression was the result of transcriptional repression mediated by interference with Foxo1 activation.

TFE3 suppresses thermogenesis in BAT

Cold exposure induces thermogenesis in BAT, thereby maintaining body temperature. We examined cold-induced thermogenesis in the WT and aP2-TFE3 mice by measuring the body temperature before and after cold exposure (4°C for 4 hours). At room temperature (RT), both strains of mice had similar body temperatures (data not shown), whereas exposure to 4°C for 4 hours caused a lower body temperature in the aP2-TFE3 Tg mice compared with that in the WT mice. This indicated that the rate of decrease in temperature was greater in the aP2-TFE3 Tg mice (Figure 7A). ATGL and Foxo1 expression in BAT was significantly lower in the aP2-TFE3 Tg mice than in the WT mice, similar to the gene expression pattern observed in WAT (Figure 7B). We next investigated the expression of genes related to thermogenesis in BAT of the WT and aP2-TFE3 Tg mice. At RT in the fasted state, the expression of UCP1 and UCP2, the genes responsible for thermogenesis, was significantly decreased in BAT from the aP2-TFE3 Tg mice (Figure 7C). The activator for these genes, PPARα, was apparently increased. Consistent with the finding at RT, the aP2-TFE3 Tg mice showed a decrease in expression of the thermogenesis genes, *UCP1*, *UCP2*, and *UCP3*, and increased levels of the activators of this expression, PPARα and PGC-1α (Figure 7D). These

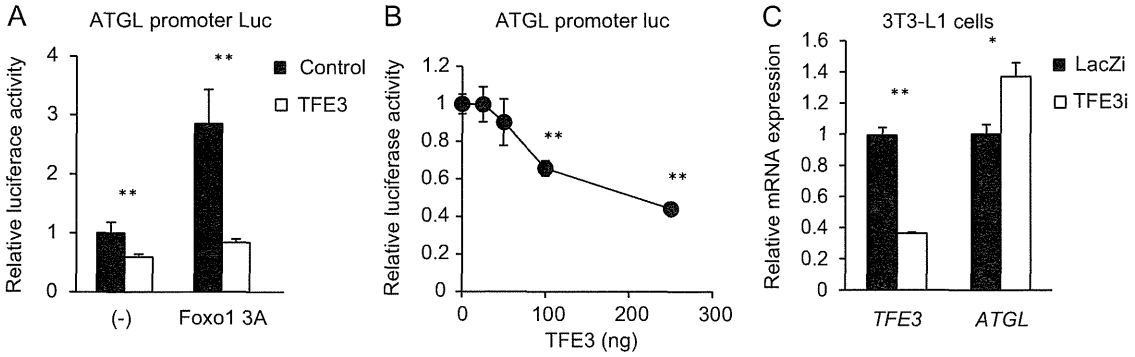

Figure 6. TFE3 suppressed ATGL promoter activity by competing with Foxo1. A, Inhibition of Foxo1 3A-induced ATGL promoter activity by TFE3 in HEK293 cells (n = 3). B, Dose-dependent effects of TFE3 on Foxo1 3A-induced ATGL promoter activity in HEK293 cells (n = 3). HEK293 cells were transfected with TFE3, Foxo1 3A, ATGL promoter luciferase constructs, and a renilla luciferase plasmid as the reference. Foxo1 3A is the phosphorylation-deficient and constitutively active mutant of Foxo1. C, The knockdown of TFE3 activated ATGL expression. 3T3-L1 cells were infected with LacZ RNAi (LacZi) or TFE3 RNAi (TFE3i) and incubated for 2 days. The expression of TFE3 and ATGL was measured by Q-PCR (n = 3). The results are expressed as means ± SEM. *, $P < .05$, **, $P < .01$ vs control or LacZi.

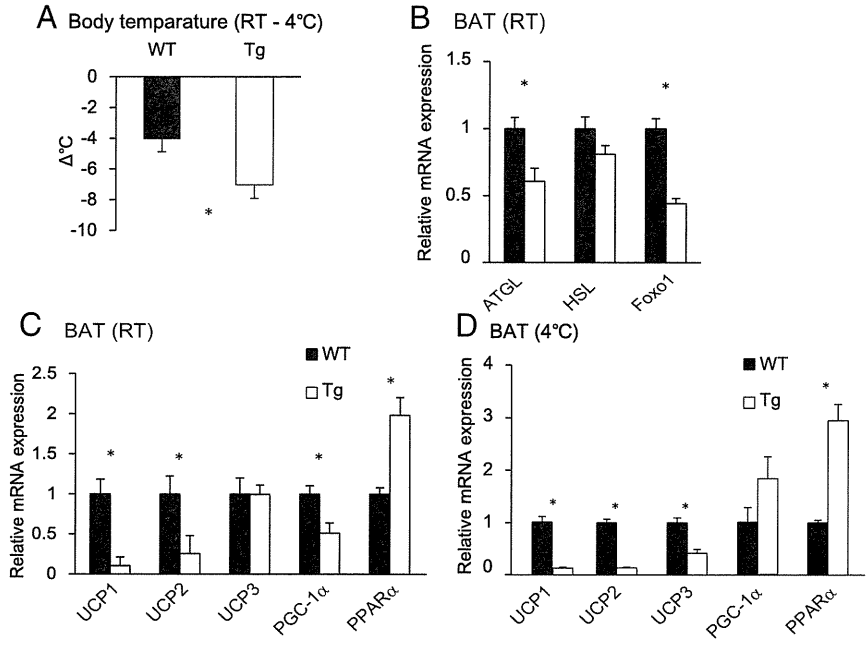

Figure 7. aP2-TFE3 Tg mice were intolerant to cold exposure. A, Eight-week-old male WT and aP2-TFE3 Tg mice were exposed to a cold temperature (4°C) for 4 hours after 17 hours of fasting. Changes in the body temperature were compared before and after cold exposure in the 2 strains of mice (n = 4). B–D, The expression of lipolysis- (B) and thermogenic (C)-related genes in BAT of 8-week-old male WT and aP2-TFE3 Tg mice after 17 hours of fasting (n = 4) (B and C), followed by cold exposure for 4 hours (n = 4) (D). The results are expressed as means ± SEM. *, $P < .05$ vs WT mice.

results indicated that the aP2-TFE3 Tg mice have impaired adaptation to cold exposure because of down-regulation of the expression of thermogenesis-related genes such as UCP1 and UCP2.

Discussion

Although TFE3 is ubiquitously expressed in tissue, its roles in regulating genes involved in metabolism are largely unknown. To date, we had proposed that TFE3 has important roles in energy homeostasis in the liver and skeletal muscle (13, 14). The expression of TFE3 is known to change in response to nutrient intake. However, the function of TFE3 in adipose tissues remains unclear. In this study, we revealed that TFE3 inhibited lipolysis in WAT by decreasing the gene expression of ATGL, the rate-limiting enzyme for lipolysis. We also showed TFE3 was involved in cold intolerance by decreasing the expression of the thermogenic genes *UCP1* and *UCP2* in BAT. Taken together these results indicate that TFE3 plays a crucial role in lipid metabolism in adipose tissues.

To examine the function of TFE3 to modulate lipid metabolism and energy expenditure in adipose tissues, including WAT and BAT of mice, we generated an adipose-specific TFE3 transgenic mouse. The weight of WAT and BAT in the aP2-TFE3 Tg mice in the fasted state was slightly but significantly increased compared with that in WT mice. Overexpression of TFE3 in the transgenic mice also increased the fasting plasma triglyceride concentration compared with that in the WT mice. These results indicated that TFE3 affected lipid metabolism in adipose tissues. Adipocyte lipolysis produces FAs as an energy source during fasting, leading us to hypothesize that TFE3 may affect lipolysis in WAT. Lipolysis activity was markedly lower in the aP2-TFE3 Tg mice than in the WT mice in both in vitro and in vivo.

β-Adrenergic signaling-stimulated lipolysis was also significantly decreased in adipocytes from the aP2-TFE3 Tg mice. Lipolysis is catalyzed by 2 lipases, including ATGL and HSL. HSL knockout mice are not obese (30, 31). Unlike HSL knockout mice, ATGL KO mice have increased deposition of TG and exhibit mild obesity (5). The whole-body and adipose-specific ATGL KO mice had markedly decreased lipolysis, indicating that ATGL plays an important role in lipolysis in WAT (4, 5). Overexpression of TFE3 in WAT also impaired the gene expression of ATGL and lipolysis under fasting conditions. There is also evidence that Foxo1 and PPARγ increase ATGL mRNA at the transcription level (29, 32), and it was recently demonstrated that IRF4 directly activates the ATGL promoter by up-regulating its expression (28). We showed that this expression of Foxo1 and IRF4 was suppressed in WAT of aP2-TFE3 Tg mice. These findings explain the decrease in ATGL mRNA in WAT of the aP2-TFE3 Tg mice.

We then verified the direct effects of TFE3 on ATGL expression. We have previously reported that TFE3 activates IRS-2 expression, resulting in the activation of insulin signaling in the liver (13). However, in contrast to these findings, TFE3 did not affect these activations in WAT (Figure 5). Therefore, TFE3 could not affect the transcriptional activity of Foxo1 regulated by insulin signaling in WAT. In luciferase analysis, TFE3 caused a significant suppression of both basal and Foxo1-induced ATGL promoter activity (Figure 6). In addition, TFE3 also down-regulated Foxo1 promoter activity in luciferase analysis (Supplemental Figure 1). These results indicated that TFE3 has a direct effect on ATGL promoter activity

and an indirect effect via a decrease in Foxo1 expression. However, there was no evidence that there are cis elements of TFE3 in the promoter regions of both the *ATGL* and *Foxo1* genes.

Several other factors have also been shown to regulate lipolysis, including CGI-58 (33), Perilipin1 (34), and G0S2 (17). Overexpression of Perilipin1 was shown to suppress lipolysis activity of ATGL (34), whereas G0S2 was reported to bind directly to ATGL, thereby inhibiting ATGL-mediated lipolysis by suppressing its TAG hydrolase activity (17). Although CGI-58 also binds to ATGL and activates lipolysis, it has been shown that G0S2 inhibits ATGL activity, even in the presence of CGI-58 (17). This indicates that G0S2 is more important than CGI-58 for regulating ATGL activity. The combined marked increase in gene expression of G0S2 and Perilipin1 that we observed in the WAT of the aP2-TFE3 Tg mice resulted in the down-regulation of ATGL enzymatic activity. These findings suggested that the decrease in lipolysis activity in WAT of aP2-TFE3 Tg mice was caused by a decrease in both ATGL gene expression and enzymatic activity.

Despite the decrease in lipolysis in the WAT of aP2-TFE3 Tg mice, plasma triglyceride and FFA levels were not decreased. Plasma FA levels represent a balance between liberation from adipose tissue and uptake by peripheral tissues. Therefore, some factors play a role in regulating the plasma lipid concentration. In fact, some studies have reported that the relationship between lipolysis and plasma lipid contents shows discrepancies in some genetically modified mice. For example, in the transcriptional regulator interacting with the PHD-bromodomain 2 (TRIP-Br2) KO mice, the plasma FFA concentration did not change despite elevated lipolysis activity in WAT (35). In addition, the aP2-ATGL Tg mice showed the same phenotypes as the TRIP-Br2 KO mice (36). Taken together, we hypothesized that the transgene is expressed in the WAT and other tissues in the aP2-TFE3 Tg mice; therefore, the transgene affected lipid metabolism including lipolysis not only in WAT but also in nonadipose tissues, leading to the unexpected results in plasma lipid concentrations observed in this study.

In addition to focusing on the functions of TFE3 in WAT, we also examined its effect in BAT. The aP2-TFE3 Tg mice were found to express the transgene in BAT as well as WAT. These mice could not maintain the body temperature during cold exposure in the fasted state (Figure 7A). Lipolysis by ATGL generates essential mediators involved in the generation of lipid ligands for PPARα activation (37). We hypothesized that cold intolerance in the aP2-TFE3 Tg mice was due to the decreased availability of FAs from WAT stores that prevented BAT function by diminishing FAs as a substrate for thermogenesis and PPARα ligands. PPARα directly regulates UCP1 gene expression, whereas PPARα/PGC-1α coordinates the control of thermogenic and lipid oxidation pathways in BAT (38). ATGL KO mice reportedly have significant decreases in *UCP1* gene expression in the liver and muscle, with the pattern of PGC-1α expression being different in these tissues (37, 39). Despite the levels of PGC-1α mRNA in BAT being higher in our aP2-TFE3 Tg mice than in WT mice in response to cold exposure, the levels of UCP1 were shown to be down-regulated. Consistent with the gene expression in WAT, ATGL and Foxo1 were decreased in BAT of aP2-TFE3 Tg mice (Figures 4A and 7B).

A previous report also showed that adipose-specific ATGL KO mice have a similar thermogenic phenotype to PPARα null mice. PPARα null mice are unable to maintain their body temperature during cold exposure (3). The supply of FAs by ATGL-catalyzed lipolysis activates PPARα to promote transcriptional activity and thermogenesis (3). The supply of FAs from both WAT to BAT and inside BAT itself was therefore suppressed in the aP2-TFE3 Tg mice, resulting in the inactivation of thermogenesis in BAT. Moreover, in the aP2-TFE3 Tg mice, the expression of thermogenic genes such as *UCP1* and *UCP2* was suppressed significantly in WAT and BAT at both RT and during cold exposure (Figures 4B, 7C, and 7D). Down-regulation of these genes may have TFE3-specific effects in BAT. These results therefore explain, in part, the mechanism underlying the reduction in body temperature observed in the aP2-TFE3 Tg mice. However, there is no evidence to date that the promoter regions of thermogenesis-related genes have cis elements, which may bind to TFE3. It is therefore necessary to determine the mechanism by which TFE3 regulates gene expression by acting as a transcription factor.

A recent clinical study showed that increased ATGL activity may contribute to elevated lipolysis and circulating FFA levels, leading to metabolic dysregulation in patients with type 2 diabetes (40). There is also evidence of decreases in mRNA and protein levels of Perilipin1 and G0S2 and increases in the ATGL protein in adipose tissues from patients with poorly controlled type 2 diabetes (40). TFE3 inhibits ATGL activity in adipose tissues by suppressing its expression and regulating the expression of regulatory molecules, including Perilipin1 and G0S2. Therefore, we consider that TFE3 has the potential to improve the metabolic syndrome by restoring insulin sensitivity as a consequence of inhibiting the synthesis of excess FAs in WAT.

Acknowledgments

We thank Enago for the English language review.

Author contributions are as follows: Y.N. and H.Sh. wrote

the manuscript; Y.F., A.Sa., K.O., A.Sh., A.N., S.Yo., and T.I. performed the experiments; Y.F., Y.N. and T.M. analyzed the data; H.I., K.K., N.Yah., M.S., S.Ya., H.Su., H.So., O.U., and N.Yam. interpreted the results of the experiments; and Y.F., Y.N., and K.O. prepared the figures.

Address all correspondence and requests for reprints to: Yoshimi Nakagawa, PhD, or Hitoshi Shimano, MD, PhD, Department of Internal Medicine (Metabolism and Endocrinology), Faculty of Medicine, University of Tsukuba, 1–1-1, Tennodai, Tsukuba, Japan 305–8575. E-mail: hshimano@md.tsukuba.ac.jp; or ynakagawa@md.tsukuba.ac.jp.

This work was supported by Grants-in-Aid from the Japanese Ministry of Science, Education, Culture, and Technology (to Y.N., H.Sh.), a grant from Takeda Science Foundation from (to Y.N.), a grant from the Novartis Foundation (Japan) for the Promotion of Science (to Y.N.), a grant from the Kowa Life Science Foundation (to Y.N.), a grant from Mochida Memorial Foundation for Medical and Pharmaceutical Research (to Y.N.), a grant from The Ichiro Kanehara Foundation for the Promotion of Medical Sciences and Medical Care (to Y.N.), a grant from the Astellas Foundation for Research on Metabolic Disorders (to Y.N.), and a grant from The Sumitomo Foundation (to Y.N.).

Disclosure Summary: The authors have nothing to disclose.

References

1. **Cannon B, Nedergaard J.** Brown adipose tissue: function and physiological significance. *Physiol Rev.* 2004;84:277–359.
2. **Karlsson M, Contreras JA, Hellman U, Tornqvist H, Holm C.** cDNA cloning, tissue distribution, and identification of the catalytic triad of monoglyceride lipase. Evolutionary relationship to esterases, lysophospholipases, and haloperoxidases. *J Biol Chem.* 1997;272:27218–27223.
3. **Ahmadian M, Abbott MJ, Tang T, et al.** Desnutrin/ATGL is regulated by AMPK and is required for a brown adipose phenotype. *Cell Metab.* 2011;13:739–748.
4. **Wei Wu J, Wang SP, Casavant S, Moreau A, Yang GS, Mitchell GA.** Fasting energy homeostasis in mice with adipose deficiency of desnutrin/adipose triglyceride lipase. *Endocrinology.* 2012;153:2198–2207.
5. **Haemmerle G, Lass A, Zimmermann R, et al.** Defective lipolysis and altered energy metabolism in mice lacking adipose triglyceride lipase. *Science.* 2006;312:734–737.
6. **Beckmann H, Su LK, Kadesch T.** TFE3: a helix-loop-helix protein that activates transcription through the immunoglobulin enhancer muE3 motif. *Genes Dev.* 1990;4:167–179.
7. **Giangrande PH, Hallstrom TC, Tunyaplin C, Calame K, Nevins JR.** Identification of E-box factor TFE3 as a functional partner for the E2F3 transcription factor. *Mol Cell Biol.* 2003;23:3707–3720.
8. **Grinberg AV, Kerppola T.** Both Max and TFE3 cooperate with Smad proteins to bind the plasminogen activator inhibitor-1 promoter, but they have opposite effects on transcriptional activity. *J Biol Chem.* 2003;278:11227–11236.
9. **Feinman R, Qiu WQ, Pearse RN, et al.** PU.1 and an HLH family member contribute to the myeloid-specific transcription of the Fc γ RIIIA promoter. *EMBO J.* 1994;13:3852–3860.
10. **Armah HB, Parwani AV.** Xp11.2 translocation renal cell carcinoma. *Arch Pathol Lab Med.* 2010;134:124–129.
11. **Betschinger J, Nichols J, Dietmann S, Corrin PD, Paddison PJ, Smith A.** Exit from pluripotency is gated by intracellular redistribution of the bHLH transcription factor Tfe3. *Cell.* 2013;153:335–347.
12. **Huan C, Kelly ML, Steele R, Shapira I, Gottesman SR, Roman CA.** Transcription factors TFE3 and TFEB are critical for CD40 ligand expression and thymus-dependent humoral immunity. *Nat Immunol.* 2006;7:1082–1091.
13. **Nakagawa Y, Shimano H, Yoshikawa T, et al.** TFE3 transcriptionally activates hepatic IRS-2, participates in insulin signaling and ameliorates diabetes. *Nature Med.* 2006;12:107–113.
14. **Iwasaki H, Naka A, Iida KT, et al.** TFE3 regulates muscle metabolic gene expression, increases glycogen stores, and enhances insulin sensitivity in mice. *Am J Physiol Endocrinol Metab.* 2012;302:E896–E902.
15. **Nakanishi N, Nakagawa Y, Tokushige N, et al** The up-regulation of microRNA-335 is associated with lipid metabolism in liver and white adipose tissue of genetically obese mice. *Biochem Biophys Res Commun.* 2009;385:492–496.
16. **Fujimoto Y, Nakagawa Y, Shingyouchi A, et al.** Dicer has a crucial role in the early stage of adipocyte differentiation, but not in lipid synthesis, in 3T3-L1 cells. *Biochem Biophys Res Commun.* 2012;420:931–936.
17. **Yang XY, Lu X, Lombes M, et al.** The G(0)/G(1) switch gene 2 regulates adipose lipolysis through association with adipose triglyceride lipase. *Cell Metab.* 2010;11:194–205.
18. **Hirota K, Daitoku H, Matsuzaki H, et al.** Hepatocyte nuclear factor-4 is a novel downstream target of insulin via FKHR as a signal-regulated transcriptional inhibitor. *J Biol Chem.* 2003;278:13056–13060.
19. **Yogosawa S, Mizutani S, Ogawa Y, Izumi T.** Activin receptor-like kinase 7 suppresses lipolysis to accumulate fat in obesity through downregulation of peroxisome proliferator-activated receptor γ and C/EBPα. *Diabetes.* 2013;62:115–123.
20. **Elmasri H, Karaaslan C, Teper Y, et al.** Fatty acid binding protein 4 is a target of VEGF and a regulator of cell proliferation in endothelial cells. *FASEB J.* 2009;23:3865–3873.
21. **Makowski L, Boord JB, Maeda K, et al.** Lack of macrophage fatty-acid-binding protein aP2 protects mice deficient in apolipoprotein E against atherosclerosis. *Nat Med.* 2001;7:699–705.
22. **Ferrell RE, Kimak MA, Lawrence EC, Finegold DN.** Candidate gene analysis in primary lymphedema. *Lymph Res Biol.* 2008;6:69–76.
23. **Urs S, Harrington A, Liaw L, Small D.** Selective expression of an aP2/fatty acid binding protein 4-Cre transgene in non-adipogenic tissues during embryonic development. *Transgen Res.* 2006;15:647–653.
24. **Cui X, Wang Y, Meng L, et al.** Overexpression of a short human seipin/BSCL2 isoform in mouse adipose tissue results in mild lipodystrophy. *Am J Physiol Endocrinol Metab.* 2012;302:E705–E713.
25. **Kamei N, Tobe K, Suzuki R, et al.** Overexpression of monocyte chemoattractant protein-1 in adipose tissues causes macrophage recruitment and insulin resistance. *J Biol Chem.* 2006;281:26602–26614.
26. **Ross SR, Graves RA, Greenstein A, et al.** A fat-specific enhancer is the primary determinant of gene expression for adipocyte P2 in vivo. *Proc Natl Acad Sci USA.* 1990;87:9590–9594.
27. **Wojciechowicz K, Gledhill K, Ambler CA, Manning CB, Jahoda CA.** Development of the mouse dermal adipose layer occurs independently of subcutaneous adipose tissue and is marked by restricted early expression of FABP4. *PloS One.* 2013;8:e59811.
28. **Eguchi J, Wang X, Yu S, et al.** Transcriptional control of adipose lipid handling by IRF4. *Cell Metab.* 2011;13:249–259.
29. **Chakrabarti P, Kandror KV.** FoxO1 controls insulin-dependent adipose triglyceride lipase (ATGL) expression and lipolysis in adipocytes. *J Biol Chem.* 2009;284:13296–13300.
30. **Fortier M, Wang SP, Mauriege P, et al.** Hormone-sensitive lipase-independent adipocyte lipolysis during beta-adrenergic stimulation, fasting, and dietary fat loading. *Am J Physiol Endocrinol Metab.* 2004;287:E282–E288.

31. **Osuga J, Ishibashi S, Oka T, et al.** Targeted disruption of hormone-sensitive lipase results in male sterility and adipocyte hypertrophy, but not in obesity. *Proc Natl Acad Sci USA.* 2000;97:787–792.
32. **Kershaw EE, Schupp M, Guan HP, Gardner NP, Lazar MA, Flier JS.** PPARγ regulates adipose triglyceride lipase in adipocytes in vitro and in vivo. *Am J Physiol Endocrinol Metab.* 2007;293:E1736–E1745.
33. **Lass A, Zimmermann R, Haemmerle G, Riederer M, Schoiswohl G, Schweiger M, Kienesberger P, Strauss JG, Gorkiewicz G, Zechner R.** Adipose triglyceride lipase-mediated lipolysis of cellular fat stores is activated by CGI-58 and defective in Chanarin-Dorfman Syndrome. *Cell Metab.* 2006;3:309–319.
34. **Miyoshi H, Souza SC, Endo M, et al.** Perilipin overexpression in mice protects against diet-induced obesity. *J Lipid Res.* 2010;51:975–982.
35. **Liew CW, Boucher J, Cheong JK, Vernochet C, et al.** Ablation of TRIP-Br2, a regulator of fat lipolysis, thermogenesis and oxidative metabolism, prevents diet-induced obesity and insulin resistance. *Nat Med.* 2013;19:217–226.
36. **Ahmadian M, Duncan RE, Varady KA, et al.** Adipose overexpression of desnutrin promotes fatty acid use and attenuates diet-induced obesity. *Diabetes.* 2009;58:855–866.
37. **Haemmerle G, Moustafa T, Woelkart G, et al.** ATGL-mediated fat catabolism regulates cardiac mitochondrial function via PPAR-α and PGC-1. *Nat Med.* 2011;17:1076–1085.
38. **Barbera MJ, Schluter A, Pedraza N, Iglesias R, Villarroya F, Giralt M.** Peroxisome proliferator-activated receptor α activates transcription of the brown fat uncoupling protein-1 gene. A link between regulation of the thermogenic and lipid oxidation pathways in the brown fat cell. *J Biol Chem.* 2001;276:1486–1493.
39. **Kienesberger PC, Pulinilkunnil T, Sung MM, et al.** Myocardial ATGL overexpression decreases the reliance on fatty acid oxidation and protects against pressure overload-induced cardiac dysfunction. *Mol Cell Biol.* 2012;32:740–750.
40. **Nielsen TS, Kampmann U, Nielsen RR, et al.** Reduced mRNA and protein expression of perilipin A and G0/G1 switch gene 2 (G0S2) in human adipose tissue in poorly controlled type 2 diabetes. *J Clin Endocrinol Metab.* 2012;97:E1348–E1352.

Prostaglandins, Leukotrienes and Essential Fatty Acids 88 (2013) 281–288

Contents lists available at SciVerse ScienceDirect

Prostaglandins, Leukotrienes and Essential Fatty Acids

journal homepage: www.elsevier.com/locate/plefa

Distinct regulation of plasma LDL cholesterol by eicosapentaenoic acid and docosahexaenoic acid in high fat diet-fed hamsters: Participation of cholesterol ester transfer protein and LDL receptor

Takayuki Ishida [a], Masahiko Ohta [a], Masanori Nakakuki [a], Hideaki Kami [a], Ryota Uchiyama [a], Hiroyuki Kawano [a,*], Tatsuto Notsu [a], Kazunori Imada [a], Hitoshi Shimano [b]

[a] Development Research, Pharmaceutical Research Center, Mochida Pharmaceutical Co., Ltd., 722 Jimba-aza-Uenohara, Gotemba, Shizuoka 412-8524, Japan
[b] Department of Internal Medicine (Endocrinology and Metabolism), Faculty of Medicine, University of Tsukuba, Ibaraki, Japan

ARTICLE INFO

Article history:
Received 26 September 2012
Received in revised form
26 December 2012
Accepted 4 January 2013

Keywords:
Eicosapentaenoic acid
Docosahexaenoic acid
Low-density lipoprotein
Cholesteryl ester transfer protein
n-3 polyunsaturated fatty acids

ABSTRACT

Despite established anti-atherogenic action, previous reports have shown that fish oils or n-3 polyunsaturated fatty acid (PUFA) increase plasma LDL-C in animals and humans. However, which component of n-3 PUFAs and what mechanisms contribute to this increase are unclear. We investigated the effects of the major components of n-3 PUFA, eicosapentaenoic acid (EPA) and docosahexaenoic acid (DHA), on plasma LDL-C in high fat diet-fed hamsters. While LDL-C increased significantly with n-3 PUFA oil and DHA, EPA had no effect on LDL-C. Interestingly, a positive correlation was found between plasma cholesterol ester transfer protein (CETP) activity and LDL-C. Only DHA increased plasma CETP activity and significantly decreased LDL receptor expression in the liver. Our data suggest that DHA, not EPA, is a major factor in the LDL-C increasing effect of n-3 PUFA oil. These differential effects on LDL-C may arise from differences in plasma CETP activity and LDL receptor expression.

1. Introduction

A lot of evidence supports the involvement of n-3 polyunsaturated fatty acids (n-3 PUFA) in reducing the risk of arteriosclerosis and coronary artery disease. These effects appear to be due to the main components of n-3 PUFA oil, eicosapentaenoic acid (EPA; 20:5 n-3) and docosahexaenoic acid (DHA; 22:6 n-3). EPA and DHA themselves possess multiple beneficial effects, including anti-inflammatory, anti-arteriosclerosis, and anti-platelet action, and are associated with inhibiting cardiovascular-related death [1,2]. Highly purified EPA in particular has been proven to inhibit the onset of cardiovascular events in a large scale clinical trial [3].

n-3 PUFA oil also possesses hypotriglyceridemic effects and has been reported to cause an increase in low-density lipoprotein cholesterol (LDL-C), which is a risk factor for coronary heart disease. In fact, multiple clinical studies report that n-3 PUFA increased LDL-C [4–6]. Of particular note is a study in which an n-3 PUFA oil preparation increased LDL-C level by 45% in patients with hypertriglyceridemia [7]. The LDL-C increasing-effect of n-3 PUFA oil has also been reported in a meta-analysis [8]. The mechanism for this LDL-C increasing-effect is not entirely clear; however, several studies have reported on the effects of n-3 PUFA oil's major components, EPA and DHA, on LDL-C level. In one clinical study, DHA alone significantly increased LDL-C level in patients with hyperlipidemia [9]. In other studies using healthy volunteers [10] or type II diabetes patients [11], however, LDL-C level did not increase, and the effect of DHA is still being debated. In contrast, EPA has had no effect on LDL-C level in these studies. From these findings, EPA and DHA may have a distinct effect on LDL metabolism, contrary to similar beneficial effects on cardiovascular disease.

Obtaining a complete understanding of the mechanism of n-3 PUFA oil-induced increase in LDL-C requires comparison of n-3 PUFA oil and its major components individually under the same experimental conditions. To date, no such report exists, however. This study investigated the effects of n-3 PUFA oil and highly purified EPA and DHA on plasma LDL-C level in hamsters, whose cholesterol metabolism is more readily comparable to that of humans than to rats and mice [12]. We found that the LDL-C increasing-effect from n-3 PUFA oil is primarily due to the effects of DHA, but not EPA, on hepatic LDL receptor (LDL-R) and plasma cholesterol ester transfer protein (CETP) activity.

2. Materials and methods

2.1. Materials

Highly purified EPA ethyl ester (EPA-E; > 98%) was obtained from Nippon Suisan Kaisha, Ltd. (Japan). Highly purified DHA

* Corresponding author. Tel.: +81 550 89 7881; fax: +81 550 89 8070.
E-mail address: h-kawano@mochida.co.jp (H. Kawano).

0952-3278/$ - see front matter © 2013 Elsevier Ltd. All rights reserved.
http://dx.doi.org/10.1016/j.plefa.2013.01.001

ethyl ester (DHA-E; >97%), ethyl oleate (OA-E; >98%) and n-3 PUFA oil (Omacor®, EPA-E 46% and DHA-E 38%) were purchased from Equateq Ltd. (Scotland), Wako Pure Chemical Industries, Ltd. (Japan) and Solvay Pharmaceuticals (Germany), respectively. Each fatty acid ethyl ester contains 0.2% alpha-tocopherol as an antioxidant. EPA-sodium salt (EPA-Na) and DHA-sodium salt (DHA-Na) were purchased from Nu-Chek Prep, Inc. (USA) and Sigma-Aldrich Co. (USA), respectively.

2.2. Animals

Six week old male Syrian hamsters (Japan SLC, Inc., Japan) were housed under controlled temperature and lighting (07:30–19:30 light, 19:30–07:30 dark cycle) with free access to water, and were assigned to the following normal and high fat diet groups: normal group (chow diet (CLEA Rodent Diet CE-2, CLEA Japan, Inc., Japan)); control group (high fat diet (D01100301, 21% (w/w) fat, 9% (w/w) sucrose, and 0.14% (w/w) cholesterol, Research Diets, Inc., USA)) supplemented with OA-E; n-3 PUFA group (Omacor®), EPA group (EPA-E) and DHA group (DHA-E). High fat diet containing 19.1% (w/w) hydrogenated coconut oil and 1.9% (w/w) safflower oil. Blood was withdrawn from non-fasted hamsters under anesthesia every 7 days. All animal experiments were carried out in accordance with Mochida Pharmaceutical's guidelines for the use and care of laboratory animals (Numbers 5522, 6079, 6411 and 6500).

2.3. Plasma isolation and determination of triglyceride, cholesterol and fatty acid composition

Blood samples were collected from the retro-orbital venous plexus of anesthetized hamsters using capillary tubes, with EDTA used as an anticoagulant. Standard enzymatic methods were used to determine plasma total cholesterol (TC), triglyceride (TG), LDL-C and high-density lipoprotein cholesterol (HDL-C) levels with commercially available kits purchased from Wako Pure Chemical Industries Ltd. Plasma CETP activity was determined by a commercial kit obtained from BioVision Inc. (USA). Plasma fatty acid composition was analyzed by gas chromatography (GC-2010AF/AOC, Shimazu Corporation, Japan). Results are shown in the Supplementary Table.

2.4. HPLC analysis of lipoprotein profiles

Plasma samples (identical volumes) were collected from all animals and pooled for each treatment group. Lipoprotein fractions in the pooled plasma were analyzed by high performance liquid chromatography (HPLC) and cholesterol content was measured. Lipoprotein fractions (chylomicron (CM), very low-density lipoprotein (VLDL), LDL and HDL) were defined by lipoprotein particle size (diameter) according to a previous study [13].

2.5. Effects of EPA and DHA on the LDL-R in HepG2 cells

Human hepatocytes (HepG2) obtained from the American Type Culture Collection (ATCC, USA) were cultured in DMEM (Sigma-Aldrich Co.) with 10% (v/v) delipidated fetal bovine serum (Nichirei, Japan). Cells were seeded in 24-well plates followed by incubation overnight with EPA-Na or DHA-Na. EPA-Na and DHA-Na were dissolved in ethanol and added to a medium containing 0.5% (w/v) bovine serum albumin (Merck KGaA, Germany) at 3–30 μM.

2.6. Effects of EPA-VLDL and DHA-VLDL on the LDL-R and LDL uptake in HepG2 cells

Syrian hamsters were fed a high fat diet (D01100301, Research Diets, Inc.) supplemented with 2% (w/w) OA-E (control), EPA-E and DHA-E for 8 days. The $d < 1.006$ g/mL lipoprotein fraction (VLDL) was prepared from pooled plasma from each group by density gradient ultracentrifugation as previously described [14]. HepG2 cells were cultured in DMEM with 10% (v/v) lipoprotein deficient fetal bovine serum (Sigma-Aldrich Co.). Cells were seeded in 24-well plates, followed by overnight incubation with VLDL (10 μg protein/mL) and LPL from bovine milk (0.5 U/mL, Sigma-Aldrich Co.). For determination of cellular LDL uptake, Dil-labeled LDL (Biomedical Technologies, Inc., USA) was added to the medium for 2 h prior to the end of incubation and the amount of cellular Dil fluorescence vs. protein concentration was determined.

2.7. Gene expression analysis

Total RNA was extracted from hamster tissues and HepG2 cells using TRIzol® Regent (Life Technologies, USA) and purified with the Purelink™ Micro-to-Midi Total RNA Purification System (Life Technologies). cDNA was generated using the SuperScript™ III First-Strand Synthesis System (Life Technologies). mRNA levels of hepatic LDL-R, fatty acid synthase (FAS), stearoyl-CoA desaturase 1 (SCD1), acetyl CoA carboxylase (ACC), sterol regulatory element binding protein (SREBP)-2 and adipose CETP were evaluated using quantitative real-time polymerase chain reaction (PCR). Quantitative real-time PCR was performed on duplicate samples using the 7500 fast real-time PCR system (Applied Biosystems, USA) with PCR Master Mix (Applied Biosystems). The relative amount of target mRNA in each sample was determined by the comparative Ct method. For each sample, mRNA levels were normalized to glyceraldehyde-3-phosphate dehydrogenase (GAPDH) or ribosomal RNA values obtained from the same samples and results were expressed relative to the control group. Oligonucleotide primers used in real-time PCR have been described in previous papers (Supplementary Table).

Gene expression in HepG2 cells was analyzed with TaqMan® Gene Expression Assay Kits (LDL-R Hs00181192_m1, GAPDH Hs02758991_g1, TaqMan® Ribosomal RNA Control Reagents (Applied Biosystems)).

2.8. Western blot analysis

Protein samples (10 μg protein/lane) from hamster livers were separated by SDS–PAGE. Western blot analysis was performed using anti-LDL-R antibody (BioVision). Anti-α-tubulin antibody (Santa Cruz Biotechnology, USA) was used as an internal control. Blots were visualized with a ECL Plus Western Blotting Detection System (GE healthcare, UK). The final result for each sample was normalized to the α-tubulin value within the same sample and the results were expressed relative to the control group.

2.9. Statistical analysis

Results are presented as mean ± S.E.M. Data were assessed using the *t*-test for two-group comparisons, Dunnett's test or Steel's test for multi-group comparison, and Spearman's correlation test for CETP activity and LDL-C correlation. A value of $P < 0.05$ was considered to be significant (*: $P < 0.05$; *: $P < 0.01$).

3. Results

3.1. Effect of n-3 PUFA oil on plasma LDL-C

High fat diet-induced plasma LDL-C level significantly increased in the presence of both 2% and 4% (w/w) n-3 PUFA oil at day 21 ($P < 0.01$; Fig. 1A). In addition, presence of 2% (w/w) n-3 PUFA oil resulted in increased cholesterol in every LDL fraction determined by HPLC (Fig. 1B).

3.2. Effect of n-3 PUFA oil on plasma TG, TC, non-HDL-C and HDL-C

Plasma TG level decreased in hamsters fed the n-3 PUFA diet compared with control. TC significantly increased with 4% (w/w) n-3 PUFA oil, and non-HDL-C significantly increased with 2% and 4% (w/w) n-3 PUFA oil at day 21 ($P < 0.05$ or $P < 0.01$), while HDL-C significantly decreased in the presence of 2% and 4% (w/w) n-3 PUFA oil ($P < 0.01$) (Table 1).

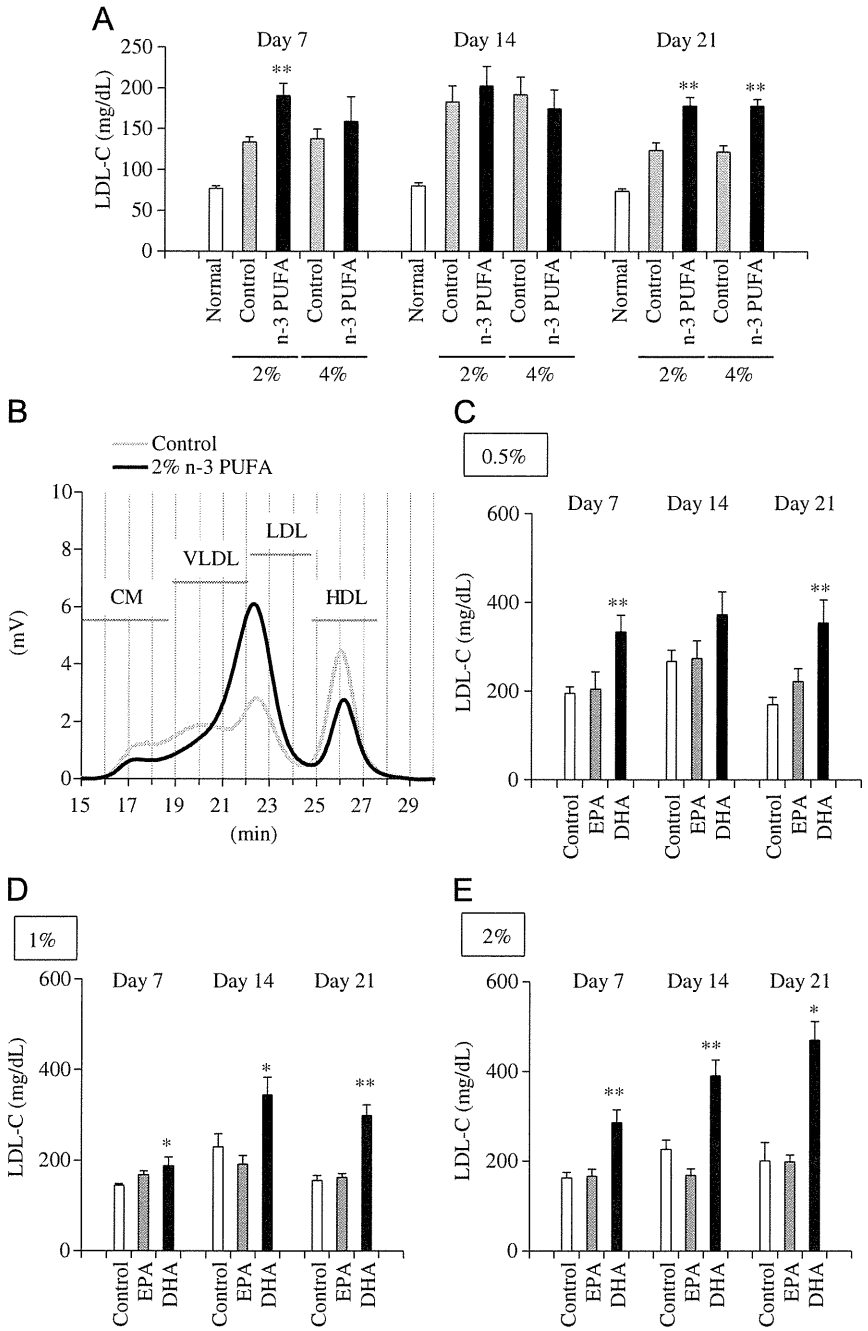

Fig. 1. Effect of n-3 PUFA oil, EPA-E and DHA-E on plasma LDL cholesterol in high fat diet-fed hamsters. (A) Plasma was prepared from hamsters fed a chow diet (normal) or a high fat diet supplemented with 2% or 4% (w/w) control (OA-E) and n-3 PUFA at day 7, 14 and 21. Values are expressed as mean ± S.E.M. of individual samples (chow group: $n=6$, high fat diet-fed group: $n=8$). (B) Identical volumes of each plasma sample from the 2% (w/w) control group and n-3 PUFA group were pooled. Cholesterol content of the samples was analyzed by HPLC. Values are expressed as the actual values. (C)–(E) Plasma was prepared from hamsters fed a high fat diet supplemented with 0.5%, 1% or 2% (w/w) control, EPA-E or DHA-E at day 7, 14 and 21. Values are expressed as mean ± S.E.M. of individual samples ($n=7$–10). $^{*}P < 0.05$, $^{**}P < 0.01$ vs. control group at every dose.